



# FGF20 Protected Against BBB Disruption After Traumatic Brain Injury by Upregulating Junction Protein Expression and Inhibiting the Inflammatory Response

Jun Chen<sup>1†</sup>, Xue Wang<sup>1†</sup>, Jian Hu<sup>1</sup>, Jingting Du<sup>1</sup>, Confidence Dordoe<sup>1</sup>, Qilin Zhou<sup>1</sup>, Wenting Huang<sup>2</sup>, Ruili Guo<sup>1</sup>, Fanyi Han<sup>1</sup>, Kaiming Guo<sup>1</sup>, Shasha Ye<sup>1\*</sup>, Li Lin<sup>1\*</sup> and Xiaokun Li<sup>1,3\*</sup>

## OPEN ACCESS

### Edited by:

Peter Vee Sin Lee,  
The University of Melbourne, Australia

### Reviewed by:

Martha Eaton O'Donnell,  
University of California, Davis,  
United States  
Dasiel Oscar Borroto-Escuela,  
Karolinska Institutet, Sweden

### \*Correspondence:

Xiaokun Li  
xiaokunli@wmu.edu.cn  
Li Lin  
linliwz@163.com  
Shasha Ye  
yeshasha0803@163.com

<sup>†</sup>These authors have contributed  
equally to this work

### Specialty section:

This article was submitted to  
Neuropharmacology,  
a section of the journal  
Frontiers in Pharmacology

**Received:** 04 August 2020

**Accepted:** 14 December 2020

**Published:** 25 January 2021

### Citation:

Chen J, Wang X, Hu J, Du J, Dordoe C,  
Zhou Q, Huang W, Guo R, Han F,  
Guo K, Ye S, Lin L and Li X (2021)  
FGF20 Protected Against BBB  
Disruption After Traumatic Brain  
Injury by Upregulating Junction Protein  
Expression and Inhibiting the  
Inflammatory Response.  
Front. Phys. 11:590669.  
doi: 10.3389/fphar.2020.590669

<sup>1</sup>School of Pharmaceutical Sciences, Wenzhou Medical University, Wenzhou, China, <sup>2</sup>School of the First Clinical Medical Sciences, Wenzhou Medical University, Wenzhou, China, <sup>3</sup>Research Units of Clinical Translation of Cell Growth Factors and Diseases Research, Chinese Academy of Medical Science, Wenzhou, China

Disruption of the blood-brain barrier (BBB) and the cerebral inflammatory response occurring after traumatic brain injury (TBI) facilitate further brain damage, which leads to long-term complications of TBI. Fibroblast growth factor 20 (FGF20), a neurotrophic factor, plays important roles in brain development and neuronal homeostasis. The aim of the current study was to assess the protective effects of FGF20 on TBI via BBB maintenance. In the present study, recombinant human FGF20 (rhFGF20) reduced neurofunctional deficits, brain edema, Evans blue extravasation and neuroinflammation in a TBI mouse model. In an *in vitro* TNF- $\alpha$ -induced human brain microvascular endothelial cell (HBMEC) model of BBB disruption, rhFGF20 reduced paracellular permeability and increased trans-endothelial electrical resistance (TEER). Both in the TBI mouse model and *in vitro*, rhFGF20 increased the expression of proteins composing in BBB-associated tight junctions (TJs) and adherens junctions (AJs), and decreased the inflammatory response, which protected the BBB integrity. Notably, rhFGF20 preserved BBB function by activating the AKT/GSK3 $\beta$  pathway and inhibited the inflammatory response by regulating the JNK/NF $\kappa$ B pathway. Thus, FGF20 is a potential candidate treatment for TBI that protects the BBB by upregulating junction protein expression and inhibiting the inflammatory response.

**Keywords:** Fgf20, traumatic brain injury, blood-brain barrier, tight junction protein, inflammatory response

## INTRODUCTION

Traumatic brain injury (TBI) is a leading cause of death and disability worldwide, particularly in children and young adults (Maiti et al., 2019; Fouda et al., 2020). TBI-induced brain damage comprises two pathological phases. Primary damage occurs at the moment of trauma (Loane and Faden, 2010), while secondary damage occurs subsequently, including excitotoxicity, blood-brain barrier (BBB) disruption, oxidative stress, neuroinflammation, ischemia, edema, etc. (Polderman, 2004). Among these processes, BBB disruption partially mediated by inflammation is a vital mechanism contributing to the progression of brain injury and long-term neurological deficits (Shi et al., 2015).

The BBB plays an important role in facilitating the transmission of neuroactive agents to regulate the brain microenvironment (Wu et al., 2020), and it is disrupted by brain edema and intracranial hypertension after TBI; indeed, BBB disruption is a major cause of death (Abbott et al., 2006). The BBB is mainly composed of cerebrovascular endothelial cells (ECs) joined tightly together by intercellular tight junction (TJ) proteins and adherens junction (AJ) proteins (Chen et al., 2018; Zhu et al., 2019). The main barrier function is provided by podocytes projecting from astrocyte, a basement membrane, pericytes, and an endothelium connected with junction proteins (Wolburg and Lippoldt, 2002). TJ and AJ proteins, including Claudin, Occludin, Zonula Occludens (ZO) and VE-cadherin, play major roles in limiting paracellular diffusion between ECs and maintaining the integrity of the BBB (Jiao et al., 2011; Zhang et al., 2020). The inflammatory reaction to TBI occurs through peripheral immune mediators produced at the entrance to the central nervous system (CNS) via a damaged BBB (Simon et al., 2017). In particular, tumor necrosis factor- $\alpha$  (TNF- $\alpha$ ), interleukin (IL)-1 $\beta$ , IL-6 and inducible nitric oxide synthase (iNOS) are crucial proinflammatory cytokines produced following trauma (Aibiki et al., 1999; Kamm et al., 2006; Villalba et al., 2014) that exacerbate and increase BBB permeability (Elwood et al., 2017). Therefore, a drug targeting BBB integrity and the inflammatory response is a potential therapeutic strategy for TBI.

Fibroblast growth factor 20 (FGF20), a member of the FGF family, is a paracrine growth factor whose orthologs are highly conserved among vertebrates. Human FGF20 is highly similar to rat FGF20 and mouse FGF20 (nearly 95% amino acid identity) (Ohmachi et al., 2000; Katoh and Katoh, 2005). According to a previous study, FGF20 is predominantly expressed in the brain (Boshoff et al., 2018), has well known neurotrophic activity (Shimada et al., 2009) and plays an important role in regulating CNS development and function (Takagi et al., 2005). The positive roles of FGF20 in Parkinson's disease (PD) imply that it may play a neuroprotective role in other CNS disorders (Niu et al., 2018). However, the effects of FGF20 on protecting BBB integrity in TBI and its possible underlying mechanism of action in regulating BBB integrity after TBI remain elusive.

Here, we aimed to determine whether recombinant human FGF20 (rhFGF20) ameliorates the pathophysiological symptoms of acute-stage TBI by preserving BBB integrity and reducing the inflammatory response. We further identified the effects of rhFGF20 on regulating the AKT/GSK $\beta$  and JNK/NF $\kappa$ B pathways and the roles of these pathways in preserving BBB integrity and inhibiting the inflammatory response.

## MATERIALS AND METHODS

### Reagents and Antibodies

The AKT inhibitor LY294002, GSK3 $\beta$  inhibitor SB216763, NF $\kappa$ B inhibitor Bay 11-7082, FITC-dextran, and Evans blue were purchased from Sigma (Sigma-Aldrich, St. Louis, MO, United States). JNK agonist anisomycin was purchased from Beyotime (Beyotime Biotechnology, Shanghai, China). TNF- $\alpha$

was obtained from R&D Systems (Minneapolis, MN, United States). The following primary antibodies were applied in this study: anti-p-GSK3 $\beta$ , anti-GSK3 $\beta$ , anti-p-JNK, anti-JNK, anti-p-NF $\kappa$ B and anti-NF $\kappa$ B antibodies purchased from Cell Signaling Technology (Danvers, MA, United States); anti-FGF20, anti-VE-cadherin, anti-Claudin-5, and anti-GFAP antibodies obtained from Abcam (Cambridge, MA, United States); and anti-p-AKT, anti-AKT and anti-Occludin antibodies purchased from Invitrogen (Carlsbad, CA, United States) and Santa Cruz Biotechnology (Dallas, TX, United States), respectively. The secondary antibodies used in this study were goat anti-rabbit immunoglobulin G (IgG) H&L (HRP) and goat anti-mouse IgG-HRP purchased from Abcam (Cambridge, MA, United States) and Santa Cruz Biotechnology (Dallas, TX, United States), respectively.

### Animals and Surgical Procedures Used to Develop a Controlled Cortical Impact (CCI)-Induced TBI Model

C57BL/6 male mice (8–12 weeks, 22–28 g) purchased from the Animal Center of the Chinese Academy of Sciences (Beijing, China) were used in this study. The animal protocols were approved by the Animal Center of the Chinese Academy of Science (Shanghai, China) and the Laboratory Animal Ethics Committee of Wenzhou Medical University.

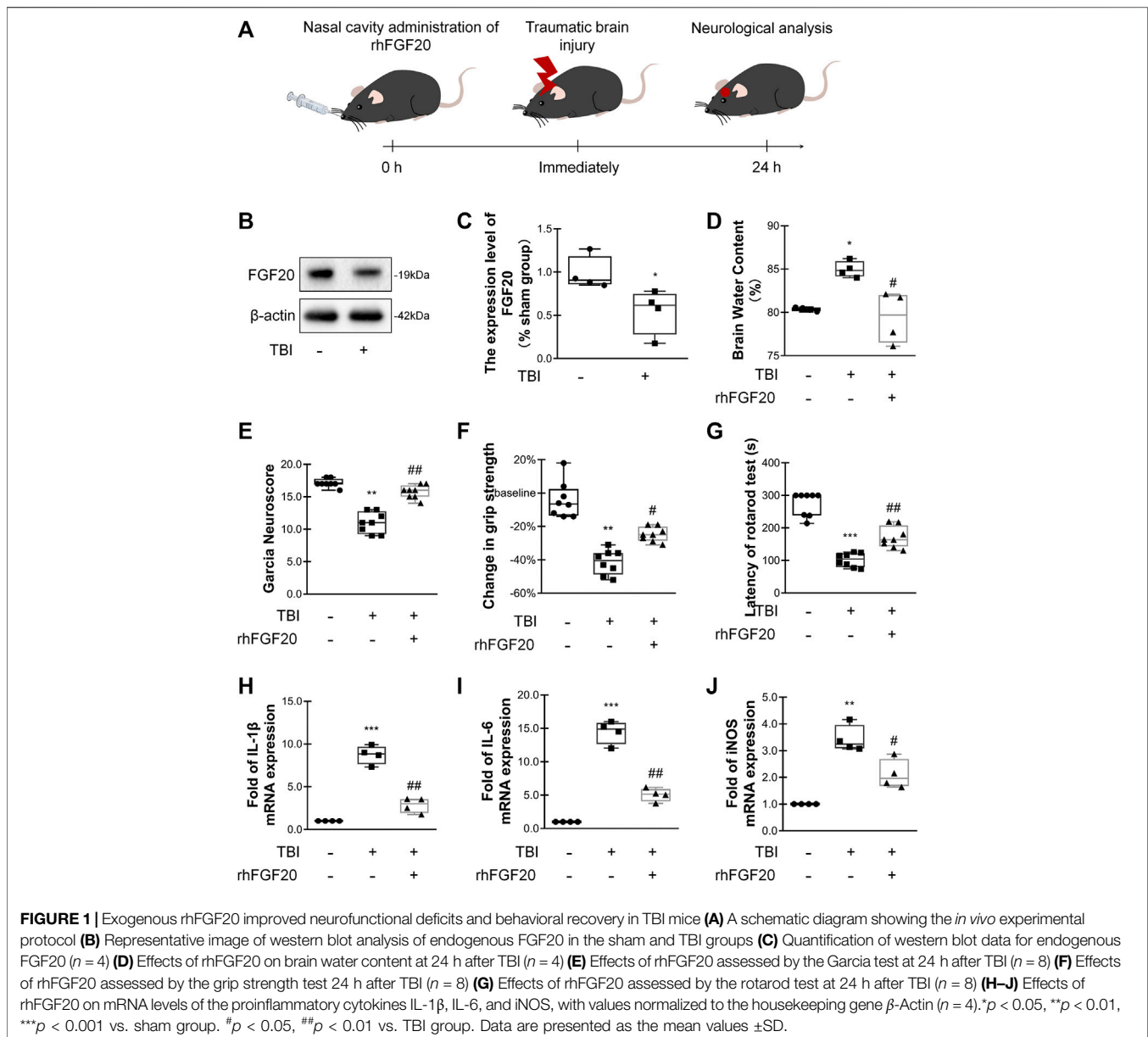
The surgical procedures were used to establish the controlled cortical impact (CCI)-induced TBI model with high reproducibility (Peterson et al., 2015). This model produces relevant clinical symptoms of TBI (Cernak, 2005). Male C57BL/6 mice were anesthetized with 4% isoflurane, administered normal saline or 0.5 mg/kg rhFGF20 by nasal delivery (Graff et al., 2005), and mounted on a stereotaxic frame for surgery to induce TBI. In brief, a 4-mm craniotomy was performed on the left parietal bone at the midpoint between the bregma and lambda sutures with the medial edge 0.55 mm lateral to the midline. The calvaria was carefully removed, and CCI injury was induced with a 3-mm diameter impactor at a rate of 3.0 m/s and a depth of 1.0 mm. After injury, the skin was sutured, and the temperature of the mouse was maintained at 37°C. Mice that underwent the craniotomy procedure but were not subjected to CCI were used as the sham group (Figure 1A).

### Rotarod Test

Mice were trained for 3 days before performing the Rotarod test. A ROTA ROD equipment (IITC Life Science) was set with the procedure that was gradually accelerated from 5 to 30 rpm over 5 min. This training procedure lasted for 3 days before sham and CCI surgery. The Rotarod test was performed in mice 24 h after Sham or CCI surgery, the rotarod latency was recorded as the time before the mouse fell off the rod or gripped the rod (Xu et al., 2018).

### Neurobehavioral Assessment

The Garcia test was conducted in mice 24 h after sham or CCI surgery under blinded conditions. Sensorimotor deficits were assessed using a modified Garcia test that included



assessments of spontaneous activity, symmetry in the movement of the four limbs, forepaw outstretching, climbing, body proprioception and response to vibrissae touch, and was scored from 0 to 18 points, with a score of 0–three points awarded for each assessment (Garcia et al., 1995).

### Grip Strength Test

The Grip strength test was conducted in mice 24 h after surgery for Sham or CCI under blinded conditions. For grip strength measurements, each mouse was suspended over a grid by the tail such that its forepaws were allowed to grasp the grid by Grip Strength Meter (UGO BASILE biological research apparatus, Italy). The mouse was then pulled backward until it released its grip. The baseline grip strength of each animal was measured

one day before CCI or the sham procedure (Glushakov et al., 2013).

### Evans Blue Extravasation

Twenty hours after sham or CCI, 0.25 ml of Evans blue dye (2% in saline) was injected intraperitoneally. Four hours after Evans blue dye injection, the anesthetized animals were transcardially perfused with saline to sufficiently remove the intravascular-localized dye and were then sacrificed. The left hemisphere was immediately weighed and homogenized in five volumes of formamide. The homogenate was incubated for 3 days at 72°C and centrifuged (15,000 rpm, 30 min). The absorbance of the supernatant was detected using a spectrophotometer (Bio-Rad, Hercules, CA, United States) at an excitation wavelength of

610 nm and an emission wavelength of 680 nm (Wang et al., 2016).

## Brain Water Content

The wet and dry weights of the brain were recorded 24 h after sham or CCI (Zhang et al., 2018). Brain tissue was obtained from mice not subjected to transcatheter perfusion. The weight of the brain tissue was measured immediately after a mouse was sacrificed and was defined as the wet weight. Subsequently, the brain was dried in an oven (100°C) for 24 h until a constant weight was achieved, and this weight was defined as the dry weight (Li et al., 2013; Genet et al., 2017). The brain water content was calculated as follow: brain water content (%) = [(wet brain weight - dry brain weight)/wet brain weight] × 100%

## Western Blot

At 24 h after CCI, mice were sacrificed and perfused with ice-cold saline solution. Brain tissue extracted from 5 mm coronal sections of the brain penumbra collected from the site of impact, and stored at -80 °C, and then were homogenized in Mammal Tissue Protein Extraction kit (Boster Biological Technology, Pleasanton, CA, United States). The cellular proteins were extracted 24 h after a TNF- $\alpha$  or rhFGF20 treatment by Culture Cellular Total Protein Extraction kit (Boster Biological Technology, Pleasanton, CA, United States). Supernatant was collected and protein levels were measured using the Quick Start Bradford 1X Dye Reagent (Bio-Rad, Hercules, CA, United States).

Equivalent amounts of protein were separated on 10 or 12% SDS-PAGE gels and then transferred to polyvinylidene fluoride (PVDF) membranes. Membranes were blocked with 5% nonfat milk in TBST for 90 min at room temperature and then incubated with the following primary antibodies overnight at 4°C: VE-cadherin (1:1,000), Occludin (1:1,000), Claudin-5 (1:800), p-AKT (1:1,000), AKT (1:1,000), p-GSK3 $\beta$  (1:1,000), GSK3 $\beta$  (1:1,000), p-NF $\kappa$ B (1:1,000), and NF $\kappa$ B (1:1,000). Membranes were subsequently incubated with the respective secondary antibodies. Finally, membranes were imaged and quantified using Image Lab 3.0 software (Bio-Rad, Hercules, CA, United States).

## Histological Analysis

Animals were anesthetized with 4% isoflurane 24 h after TBI. The whole brain was post-fixed with 4% paraformaldehyde for 12 h and embedded in paraffin. Transverse sections (5- $\mu$ m thick) were mounted on slides for subsequent staining. Hematoxylin and eosin (H&E) and Nissl staining were performed to observe histopathological changes according to the manufacturer's protocol (Vigo et al., 2019). Images were acquired using a light microscope.

Immunofluorescence staining was performed to detect protein expression. For *in vivo* protein detection, sections were deparaffinized, rehydrated, and incubated with 5% bovine serum albumin (BSA) to block nonspecific binding. Then, sections were incubated with primary antibodies overnight at 4°C. The following primary antibodies were applied: VE-cadherin (1:300), Occludin (1:300), Claudin-5 (1:300), Iba-1 (1:100), and glial fibrillary acidic protein GFAP (1:300). For the negative

**TABLE 1** | Primers' sequences used for real-time PCR analysis.

Gene	Sequence 5'-3'	Amplification length (bp)
IL-1 $\beta$ (mouse)	AAGCCTCGTGTGTCGGACC TGAGGCCCAAGGCCACAGGT	140
TNF- $\alpha$ (mouse)	CAAGGGACAAGGCTGCCCG GCAGGGGCTCTTGACGGCAG	109
IL-6 (mouse)	AGAAGGAGTGGCTAAGGACCAA AACGCACTAGGTTTGCCGAGTA	101
$\beta$ -Actin (mouse)	CACTGCAAACGGGGAATGG TGAGATGGACTGTCGGATGG	198
IL-1 $\beta$ (human)	GCCCTAAACAGATGAAGTGCTCCT CCTGAAGCCCTTGCTGTAGTG	104
TNF- $\alpha$ (human)	GTGACAAGCCTGTAGCCCA ACTCGGCAAAGTCGAGATAG	414
IL-6 (mouse)	ACTCACCTCTTCAGAACGAATTG CCATCTTTGGAAGGTTTCAGGTTG	149
$\beta$ -Actin (human)	AGCACAATGAAGATCAAGAT TGTAACGCAACTAAGTCATA	188

control slides, primary antibody was replaced with 1% BSA. The sections were incubated with Alexa Fluor 488-conjugated secondary antibodies (1:500) for 1 h at room temperature. Then the nuclei were stained with DAPI. The stained sections were imaged using a Nikon ECLIPSE 80i fluorescence microscope (Nikon, Japan). No immunoreactive cell was observed in the negative control slides.

ImageJ (NIH, United States) was used to automatically determine the fluorescence intensity, Soma area and process length of microglia (Iba-1<sup>+</sup> cells) and astrocytes (GFAP<sup>+</sup> cells) from microscopic fields randomly selected from the peri-injury regions of four animals per group.

## RNA Extraction and RT-PCR

Total RNA was extracted from 5-mm brain coronal sections prepared from the site of impact or HBMECs using the TriPure Isolation Reagent (Roche, South San Francisco, CA, United States). The RNA concentration was quantified by NanoDrop spectrophotometer (Thermo Fisher Scientific, MA, United States). One microgram of RNA was used to synthesize cDNAs with the PrimeScript RT Reagent Kit (RR037A, TaKaRa, Japan), and then PCR was conducted with the SYBR Green PCR Master Mix (Bio-Rad, Hercules, CA, United States). The oligonucleotide PCR primer pairs are listed in **Table 1**, purchased from Sango Biotech (Shanghai, China). The relative quantity in each sample was normalized to the level of  $\beta$ -Actin mRNA expressed. The results are presented as the means  $\pm$  SEMs of duplicate samples from three independent experiments.

## Cell Culture and *in vitro* BBB Disruption Model

Primary human brain microvascular endothelial cells (HBMECs; ACBRI376, Cell Systems Corporation, Kirkland, WA) were cultured in endothelial cell basal medium-2 (EBM-2) and plated in 6-mm wells or 24-well Transwell inserts coated with collagen I. The plates were incubated at 37°C in a humidified

atmosphere containing 5% CO<sub>2</sub>. Recombinant human TNF- $\alpha$  was used to establish the BBB disruption model (Rochfort and Cummins, 2015). Cells at a confluence of approximately 90% were treated with TNF- $\alpha$  (50 ng/ml), rhFGF20 (50 nM) or in combination with the AKT inhibitor LY294002 (20  $\mu$ M) (Wang et al., 2016), the GSK3 $\beta$  inhibitor SB216763 (30  $\mu$ M) (Li et al., 2015), the JNK agonist anisomycin (4  $\mu$ M) (Li et al., 2012), or the NF $\kappa$ B inhibitor Bay11-7082 (5  $\mu$ M) (Odobasic et al., 2019) for 24 h and were then harvested for further analysis.

### FITC-Dextran Permeability

HBMECs were cultured at a density of  $1 \times 10^5$  cells/well on polycarbonate 24-well Transwell insert chambers with 0.4-mm pores. After 2 days, cells had proliferated and reached compact density, and then were treated with or without TNF- $\alpha$  and rhFGF20. After 24 h, the medium from the Transwell inserts was replaced with new medium containing 0.1 mg/ml of fluorescein isothiocyanate (FITC)-labeled dextran (MW, 70,000; Sigma, St. Louis, MO). After 4 h, the fluorescence of each well was detected with spectrophotometer (Bio-Rad, Hercules, CA, United States) at an excitation wavelength of 485 nm and an emission wavelength of 520 nm (Zhao et al., 2019).

### Trans-endothelial Electrical Resistance (TEER)

TEER indicating the permeability of the HBMEC monolayer was measured with an EVOM resistance meter (World Precision Instruments, Sarasota, FL) according to the operation manual. Twenty-four-well Transwell inserts (6.5 mm, 0.4-mm pores) with cultured HBMECs were transferred to a chamber containing 0.1 M KCl based on a previous study (Lin et al., 2018). Then, the culture medium in the Transwell insert was replaced with 0.1 M KCl. The chamber and Transwell insert were connected through an EndOhm connector cable. The resistance was then measured with the EVOM resistance meter, and the TEER value was multiplied by the total membrane surface area to obtain the resistance value in  $\Omega \cdot \text{cm}^2$ . A blank Transwell chamber without HBMECs was used as the blank control (Zhao et al., 2019).

### Statistical Analysis

GraphPad Prism software (GraphPad Software, Inc., San Diego, CA) was used to analyze the data. Statistically significant differences among data from three or more groups were evaluated using one-way analysis of variance (ANOVA) followed by the Tukey-Kramer test.  $p < 0.05$  was considered statistically significant.

## RESULT

### rhFGF20 Treatment Improved Neurofunctional and Behavioral Recovery in Mice After TBI

In order to assess the relationship between FGF20 expression and acute-stage TBI, we investigated the levels of FGF20 protein in the

mouse brain. Compared with the sham group, the FGF20 level in the brain of the TBI group was significantly reduced (Figure 1B,C). These data suggested that FGF20 has a certain correlation with TBI.

We assessed the degree of brain edema following TBI by analyzing the brain water content. The brain water content was significantly decreased in mice in the rhFGF20 treatment group compared to mice in the TBI group 24 h after TBI (Figure 1D). After TBI, the neurological function of the mice was severely damaged. We then investigated whether rhFGF20 promoted behavioral recovery following TBI. The Garcia test was used to assess neurofunctional deficits in mice with TBI (Garcia et al., 1995). Mice exhibited neurofunctional deficits after TBI, and rhFGF20 administration markedly ameliorated these neurofunctional deficits (Figure 1E). The grip strength test was used to assess forelimb function (Glushakov et al., 2013). Mice in the TBI group exhibited functional deficits in forelimb strength; however, administration of rhFGF20 diminished these functional deficits (Figure 1F). The rotarod test measures motor coordination in mice. Latency in the rotarod test was decreased in mice in the TBI group, whereas rhFGF20 clearly increased the latency (Figure 1G). These results indicated that exogenous rhFGF20 ameliorated neurofunctional deficits, increased forelimb strength, reduced motor coordination behavioral deficits and decreased the degree of cerebral edema after TBI.

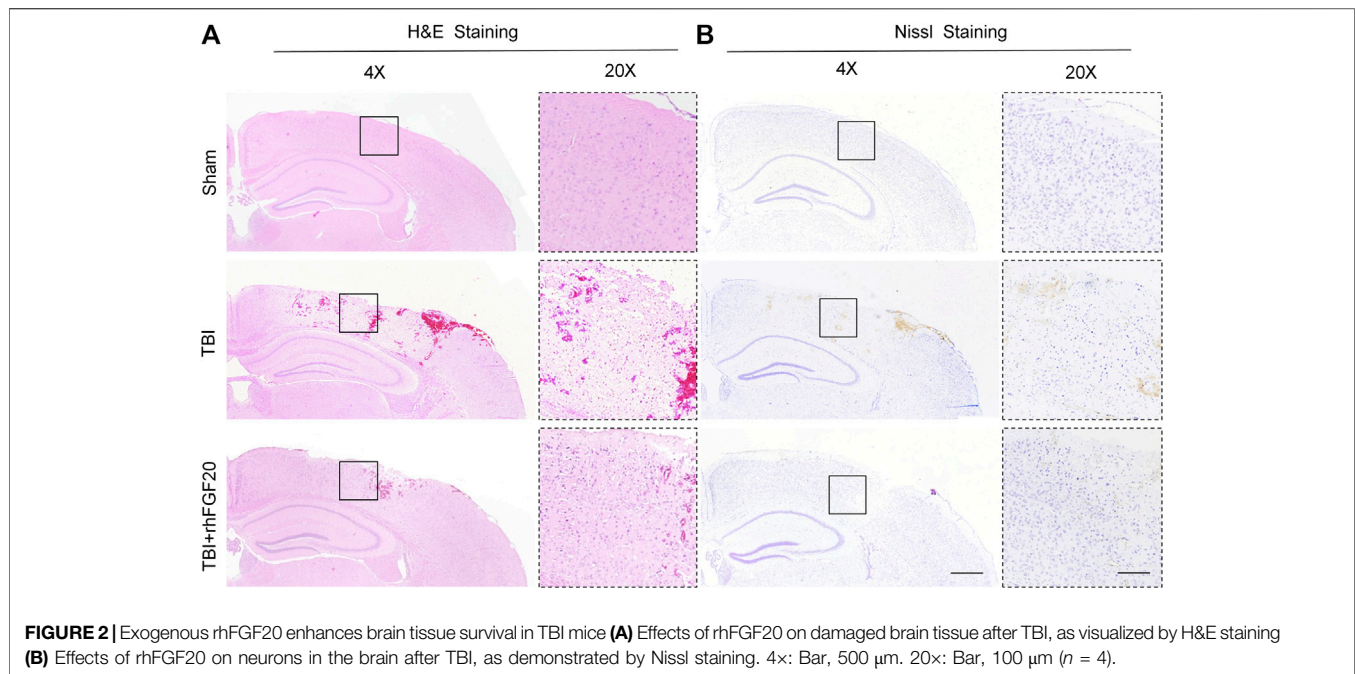
### rhFGF20 Inhibited the Inflammatory Response After TBI

TBI induces an inflammatory response that increases the levels of several inflammatory factors, producing further damage. To evaluate the anti-inflammatory effect of rhFGF20 after TBI, we examined the levels of the proinflammatory cytokines IL-1 $\beta$ , IL-6 and the proinflammatory enzyme iNOS after TBI.

The expression levels IL-1 $\beta$ , IL-6, and iNOS were measured using RT-PCR. The administration of rhFGF20 significantly reduced the expression of these proinflammatory cytokines after TBI (Figure 1H-J). Based on the data presented above, we postulated that the rhFGF20 treatment inhibited inflammation and protected against BBB disruption after TBI.

### rhFGF20 Treatment Improved Brain Tissue Survival in Mice Following TBI

Furthermore, Hematoxylin-eosin (H&E) staining and Nissl staining of brain sections were performed to assess the effect of rhFGF20 on the brain tissue and neurons. H&E staining revealed the cells in the brain tissue of the sham group mice were arranged neatly and the cytoplasm of the cells was abundant. However, many pyknotic cells were observed in the brain tissue of TBI-induced mice. In addition, the cytoplasm presented light coloring. While rhFGF20 administration partially ameliorated these abnormalities (Figure 2A). In addition, Nissl staining showed that rhFGF20 decreased neuronal loss after TBI (Figure 2B).



### rhFGF20 ameliorated TBI-Induced BBB Disruption and Increased the Expression of Junction Proteins

Evans blue dye can leak through the damaged BBB and remain in the cortex, and Evans blue extravasation experiments can elucidate the degree of BBB disruption (Chen et al., 2017). Compared with the sham group, Evans blue dye extravasation was significantly increased in the TBI group, while treatment with rhFGF20 dramatically reduced leakage (Figure 3A,B), indicating that rhFGF20 ameliorated TBI-induced BBB damage.

TJ and AJ proteins are important mediators of BBB integrity. To elucidate the effect of rhFGF20 on TJ and AJ proteins, we determined junction protein levels after TBI via western blot analysis and immunofluorescence staining. Western blot analysis revealed significantly decreased levels of VE-cadherin, Occludin and Claudin-5 after TBI. In contrast, rhFGF20 markedly increased the levels of these proteins (Figure 3C-F). The results of immunofluorescence staining were consistent with the western blotting data (Figure 3G). These data indicated that rhFGF20 treatment protected against BBB disruption after TBI and increased the expression of TJ and AJ proteins.

### rhFGF20 Inhibited Neuroinflammation and Suppressed Glial Activation After TBI

Activation of microglial and astrocytes activation, a key manifestation of CNS neuroinflammation (Schober et al., 2019), was assessed using immunofluorescence labeling to determine the cell number, soma area, and process length. TBI clearly activated Iba1-positive microglia in the cortex, as indicated by the increased soma area compared with those in the sham group. However, rhFGF20 treatment inhibited

neuroinflammation by reducing the number of activated microglia and soma area, however, microglial process length was not significantly affected (Figure 4A-D). In addition, TBI greatly increased the number of activated GFAP-positive cells in the cortex and the number of branches, while rhFGF20 treatment significantly decreased the population of activated astrocytes and the number of their branches (Figure 4E-G).

### rhFGF20 Improved Recovery After TBI via the AKT/GSK3 $\beta$ and JNK/NF $\kappa$ B Signaling Pathways

In the current study, to investigate the mechanism underlying the protective effect of rhFGF20 after TBI, we evaluated downstream pathway proteins. According to a previous study, the TBI-induced decrease in junction protein levels correlates with the AKT pathway (Wang et al., 2016). Our data showed that rhFGF20 administration significantly reversed the TBI-induced decrease in the phosphorylation of AKT and GSK3 $\beta$ , however, the expression level of total AKT and total GSK3 $\beta$  didn't obviously changed. (Figure 5A-E). These data suggested that AKT/GSK3 $\beta$  are probably involved in the protective effect of rhFGF20 on the BBB.

JNK plays an important role in inflammatory diseases (Zhou et al., 2019) and the transcription factor NF $\kappa$ B also is a major regulator of inflammation. Activation of JNK was determined by monitoring its phosphorylation. In addition, NF $\kappa$ B pathway activation was assessed by detecting the level of its phosphorylation. We detected the activation levels of JNK and NF $\kappa$ B in our study. In mice subjected to TBI, the levels of JNK phosphorylation and NF $\kappa$ B phosphorylation were both increased. However, rhFGF20 decreased the levels of *p*-JNK and *p*-NF $\kappa$ B after TBI, while both TBI surgery and FGF20 administration did not significantly affect the total expression level of JNK and NF $\kappa$ B

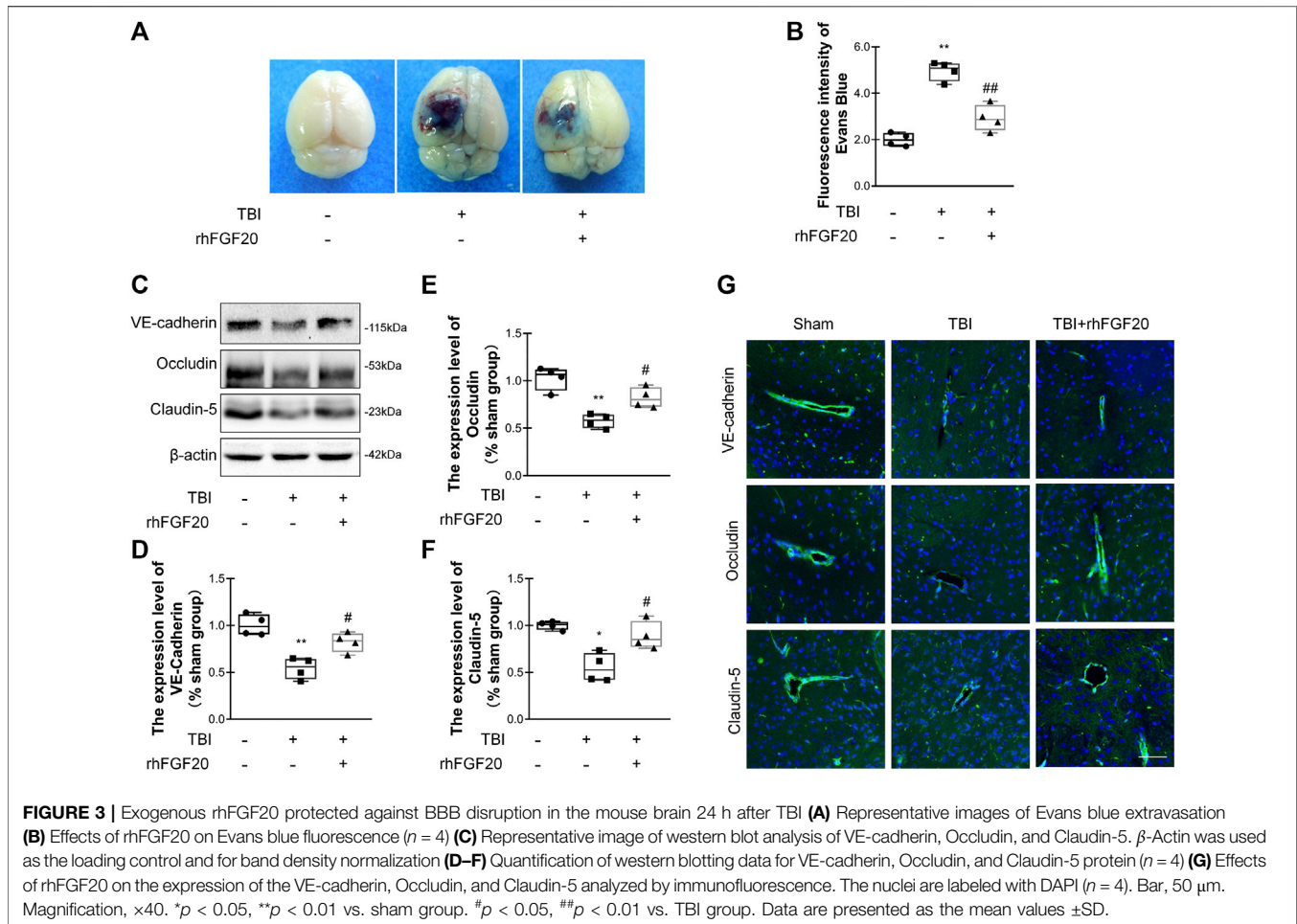


(Figure 5F–J). These data suggest that JNK/NF $\kappa$ B is probable involved in the anti-inflammatory effect of rhFGF20.

### rhFGF20 Protected Against TNF- $\alpha$ -Induced BBB Injury

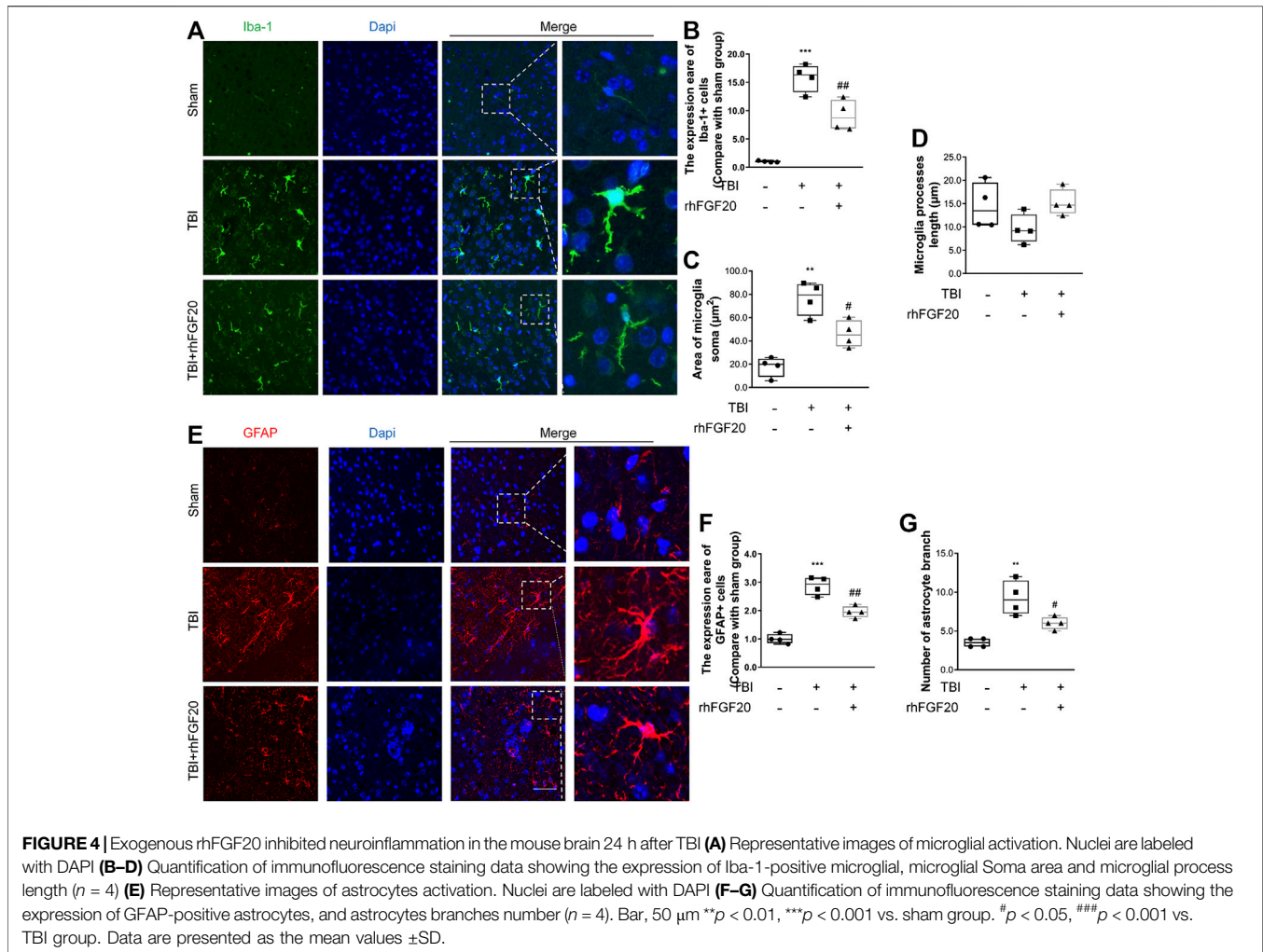
The most important component and functional unit of BBB is endothelial cells. The TNF- $\alpha$ -induced BBB injury model on HBMEC was specifically used in this study for the protective effect of rhFGF20 in ECs, and then verified that our previous conjecture that FGF20 can repair the BBB injury and its specific mechanism.

To show the paracellular permeability of ECs, FITC-dextran permeation through the monolayer was assessed, and TEER experiments were performed. The TNF- $\alpha$  group showed a high degree of FITC-dextran permeation degree and low resistance, indicating that the barrier integrity was severely damaged. However, rhFGF20 treatment clearly reduced FITC-dextran permeation and ameliorated the decrease in resistance (Figure 6A,B). In addition, the results of the Cell Counting Kit-8 (CCK8) cell viability assay suggested that TNF- $\alpha$  and rhFGF20 did not regulate the cell survival rate (Figure 6C). Therefore, the effect of rhFGF20 on the TNF- $\alpha$ -induced disruption of endothelial

monolayer permeability was mediated by treating damaged cells rather than increasing the number of cells. We postulate that the TNF- $\alpha$ -induced cellular model of BBB disruption used in our study was a reasonable approach and that rhFGF20 treatment ameliorated TNF- $\alpha$ -induced endothelial barrier damage. The expression levels of IL-1 $\beta$ , IL-6 and iNOS were significantly increased in TNF- $\alpha$ -induced HBMECs; however, rhFGF20 exerted an anti-inflammatory effect on TNF- $\alpha$ -induced HBMECs by decreasing the levels of these inflammatory factors (Figure 6D–F).

### rhFGF20 Protected Against TNF- $\alpha$ -Induced BBB Injury by Increasing Junction Protein Expression

TJ and AJ proteins are important regulators of paracellular permeability in ECs. Therefore, we detected the levels of TJ and AJ proteins in HBMECs. TNF- $\alpha$  significantly decreased the levels of VE-cadherin, Occludin and Claudin-5; however, rhFGF20 increased the levels of these proteins (Figure 7A–D). The results of immunofluorescence staining were consistent with the western blotting. TNF- $\alpha$  significantly decreased the levels of these junction proteins in the membrane, whereas rhFGF20



administration dramatically rescued the levels of these proteins (Figure 7E–H).

### rhFGF20 Protected Against TNF- $\alpha$ -Induced BBB Injury by Activating the AKT/GSK3 $\beta$ Signaling Pathway

We evaluated whether the effects of rhFGF20 on TNF- $\alpha$ -induced BBB injury were mediated by the AKT/GSK3 $\beta$  pathway. Consistent with the *in vivo* results, rhFGF20 significantly rescued the TNF- $\alpha$ -induced decrease in AKT phosphorylation. And the expression level of total AKT didn't observably changed after TNF- $\alpha$  treatment or rhFGF20 treatment (Figure 8A–C). The AKT inhibitor LY294002 was administered with rhFGF20 to determine whether the protective effect of rhFGF20 on the BBB observed in our study is related to AKT. LY294002 not only significantly reversed the effect of rhFGF20 on restoring BBB permeability and endothelial resistance (Figure 8D,E) but also decreased the expression of Claudin-5 (Figure 8F,G). We further assessed the effect of rhFGF20 downstream of AKT and found that LY294002 significantly inhibited the rhFGF20-induced increase in the level of *p*-GSK3 $\beta$  but not total GSK3 $\beta$  (Figure

8H–J). The GSK3 $\beta$  inhibitor SB216763 also reversed the protective effect of rhFGF20 on permeability and endothelial resistance (Figure 8K–L). These results further confirmed that rhFGF20 protected against TNF- $\alpha$ -induced BBB injury by activating the AKT/GSK3 $\beta$  signaling pathway.

### rhFGF20 Protected Against TNF- $\alpha$ -Induced BBB Injury by Inhibiting the Inflammatory Response Mediated by the JNK/NF $\kappa$ B Signaling Pathway

In addition, we investigated the anti-inflammatory mechanism by which rhFGF20 protects against BBB injury. The JNK signaling pathway is important for endothelial inflammation (Lu et al., 2019). Consistent with the *in vivo* results, rhFGF20 significantly decreased the TNF- $\alpha$ -induced increase in JNK phosphorylation, but did not affect the expression level of total JNK (Figure 9A–C). Furthermore, we used the JNK agonist anisomycin in our study. Anisomycin not only significantly reversed the effect of rhFGF20 on restoring the BBB permeability and endothelial resistance (Figure 9D,E) but also increased the level of the IL-1 $\beta$ , IL-6 and iNOS mRNAs (Figure 9F–H). The downstream targets in the

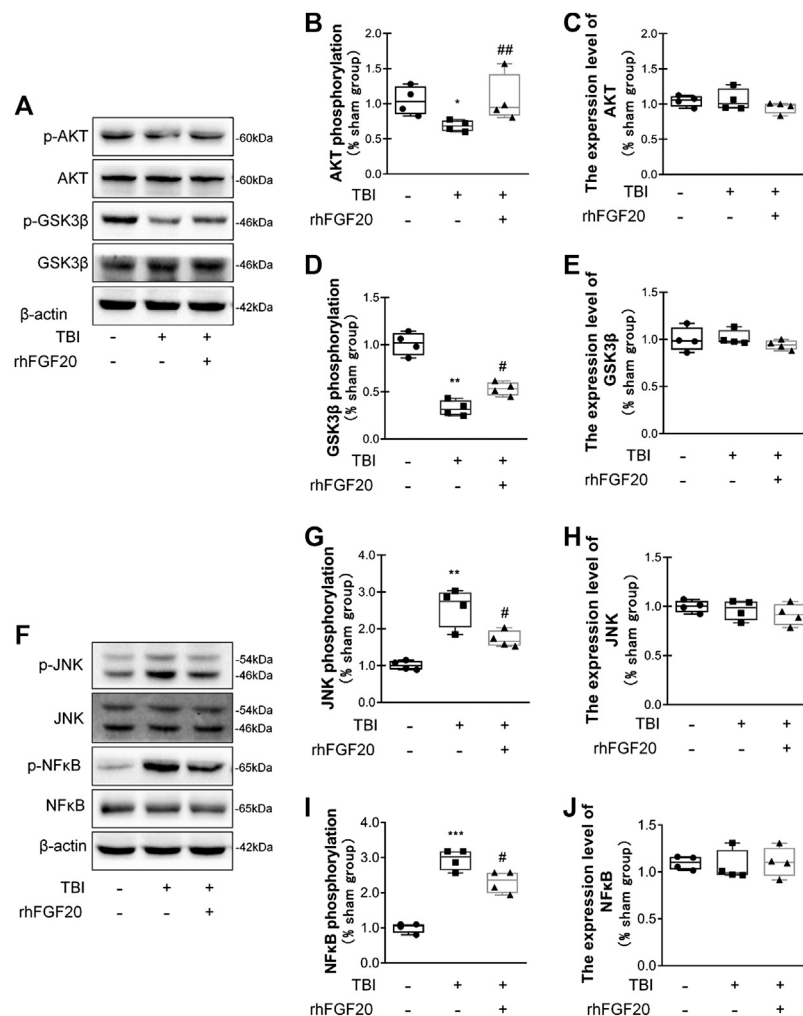
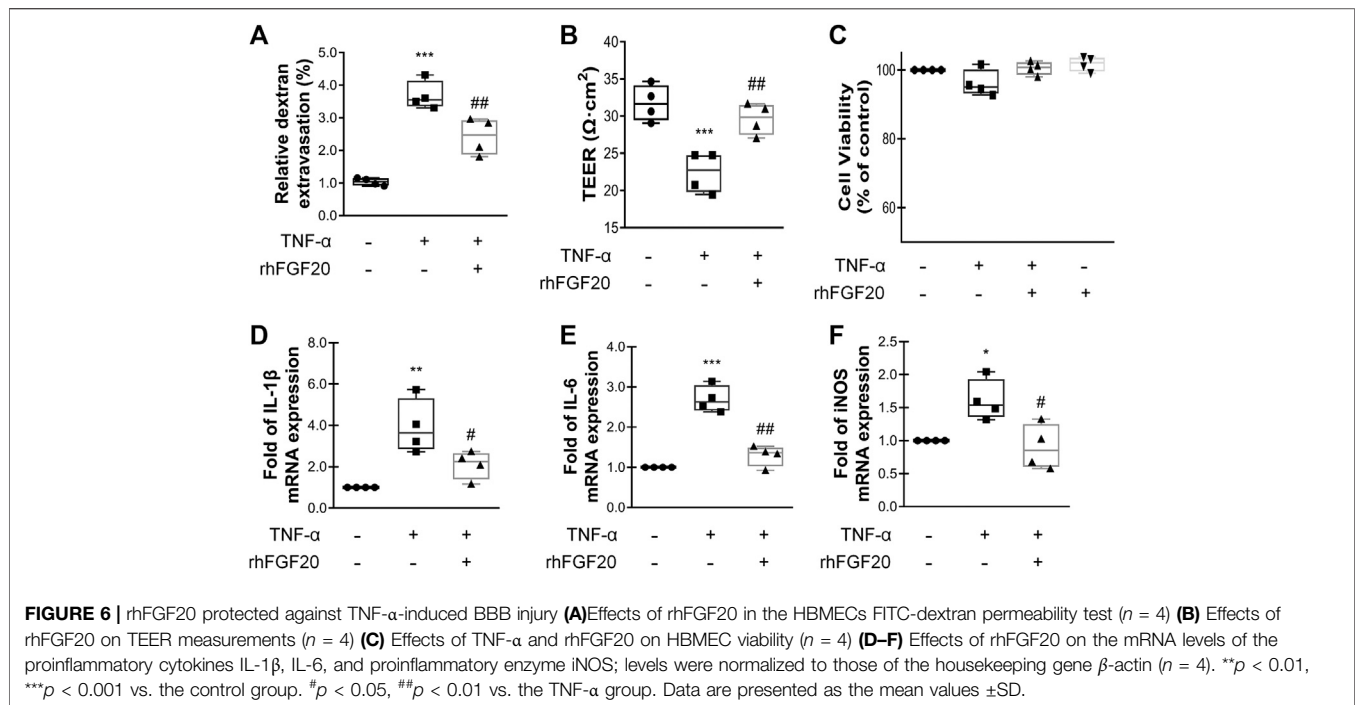


**FIGURE 5 |** Exogenous rhFGF20 improved recovery after TBI via the AKT/GSK3 $\beta$  and JNK/NF $\kappa$ B signaling pathways **(A)** Representative image of western blot analysis of p-AKT, AKT, p-GSK3 $\beta$  and GSK3 $\beta$  in the mouse brain 24 h after TBI **(B–E)** Effects of rhFGF20 on p-AKT, AKT, GSK3 $\beta$  and p-GSK3 $\beta$  protein levels, as analyzed by quantification of western blot data ( $n = 4$ ) **(F)** Representative images from western blot analysis of p-JNK, JNK, p-NF $\kappa$ B and NF $\kappa$ B.  $\beta$ -Actin was used as the loading control and for band density normalization **(G–J)** Effects of rhFGF20 on the p-JNK, JNK, p-NF $\kappa$ B and NF $\kappa$ B protein levels, as analyzed by quantification of western blotting data ( $n = 4$ ). \* $p < 0.05$ , \*\* $p < 0.01$ , \*\*\* $p < 0.001$  vs. sham group. # $p < 0.05$ , ## $p < 0.01$  vs. the TBI group. Data are presented as the mean values  $\pm$ SD.

JNK signaling pathway include various transcription factors. The transcription factor NF $\kappa$ B is a major regulator of inflammation. We speculated that NF $\kappa$ B is a downstream factor in the JNK pathway. We further assessed the anti-inflammatory effects of rhFGF20 downstream of JNK and found that anisomycin significantly inhibited the rhFGF20-induced decrease in NF $\kappa$ B phosphorylation and nuclear translocation, but did not significantly affect the total NF $\kappa$ B expression, as detected using both western blotting and immunofluorescence staining (**Figure 10A–D**). The NF $\kappa$ B inhibitor Bay 11–7082 was applied to examine the effect of NF $\kappa$ B on endothelial monolayer permeability. Bay 11–7082 also reversed the TNF- $\alpha$ -induced injury to BBB permeability and endothelial resistance (**Figure 10E,F**). These results further confirmed that rhFGF20 protected against TNF- $\alpha$ -induced BBB injury by decreasing the inflammatory response mediated by the JNK/NF $\kappa$ B signaling pathway.

## DISCUSSION

BBB dysfunction occurs within hours or days after TBI and contributes to secondary injury processes, such as edema, cell death, and neuroinflammation, as well as to the severity of the injury (Main et al., 2018). BBB breakdown can be a therapeutic target in TBI treatment (Shlosberg et al., 2010). In the current study, we confirmed that exogenous administration of rhFGF20 upregulated the expression of TJ and AJ proteins VE-cadherin, Occludin and Claudin-5, protected against BBB disruption, decreased the degree of cerebral edema, thereby ameliorating functional behavior deficits after TBI. In addition, *in vitro* TNF- $\alpha$ -induced HBMECs were established to model BBB disruption. Similarly, rhFGF20 upregulated the expression of the TJ and AJ proteins, and ameliorated the TNF- $\alpha$ -induced increase in HBMEC permeability. Both the *in*



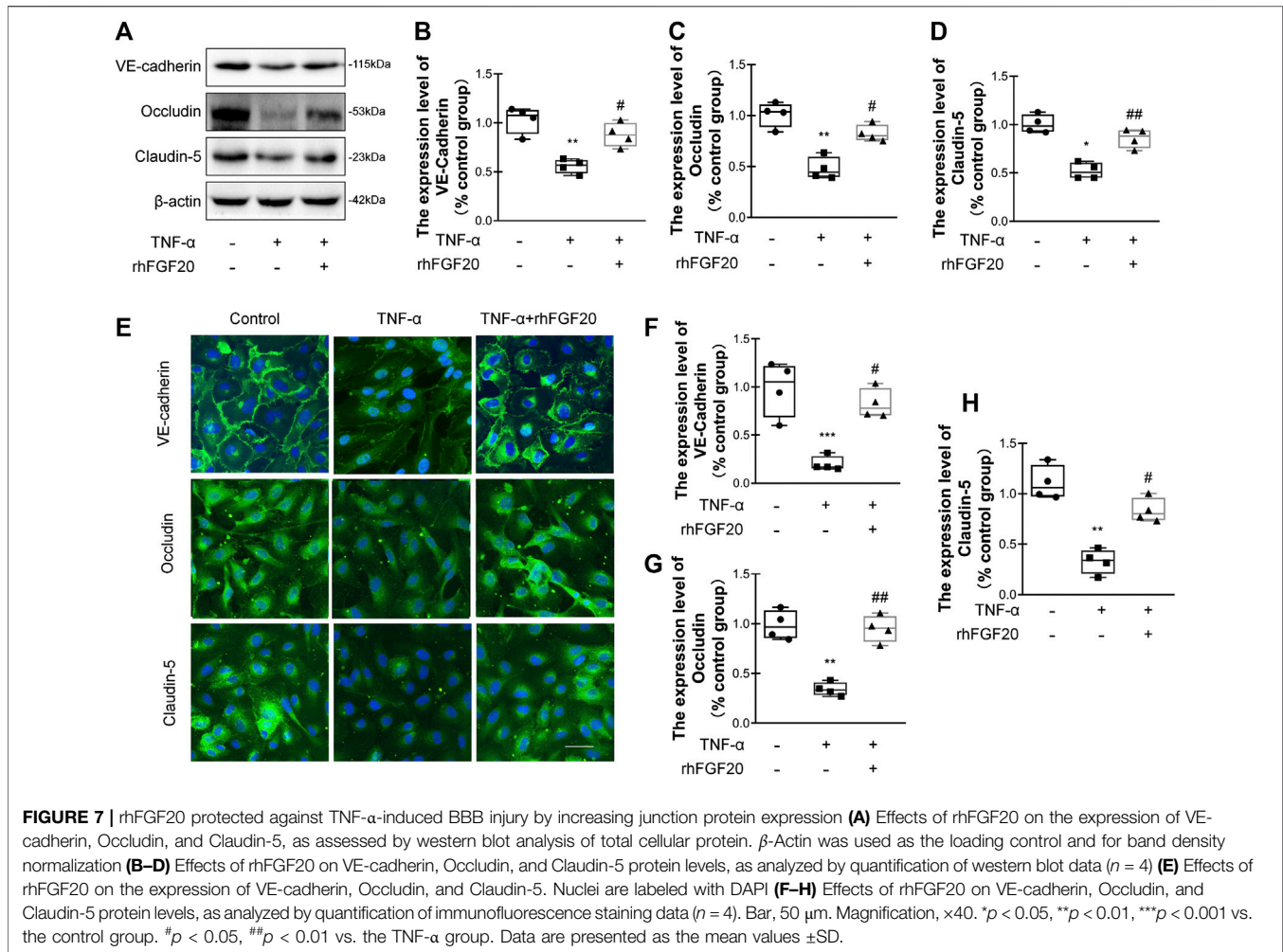
*vivo* and *in vitro* studies demonstrated that rhFGF20 upregulated the expression of TJ and AJ proteins and protected against BBB disruption by activating the AKT/GSK3 $\beta$  pathway. In addition, exogenous administration of rhFGF20 inhibited inflammation in ECs through the JNK/NF $\kappa$ B signaling pathway. These data demonstrated that rhFGF20 might be useful as a therapeutic agent for BBB protection and TBI treatment (Figure 11).

Emerging studies have demonstrated that FGFs have positive effects after TBI. Overexpression of FGF2 promoted neurogenesis and protected neurons against degeneration in the hippocampus of adult mice after TBI (Yoshimura et al., 2003). Exogenous administration of FGF2 has been reported to attenuate histopathological damage and improve functional outcomes after TBI (Yan et al., 2000). Mesenchymal stem cells (MSCs) overexpressing FGF21 (MSC-FGF21) transplanted to mouse brain by intracerebroventricular injection have been shown to significantly alleviate TBI-induced spatial memory deficits, and enhanced hippocampal neurogenesis (Shahrer et al., 2020). In our previous study, rhFGF21 administration markedly upregulated TJ and AJ protein expression, preserved BBB integrity, and reduced neurofunctional behavior deficits and cerebral edema in a mouse model after TBI (Chen et al., 2018). The present study is the first to reveal the capacity of FGF20 to preserve the BBB after TBI and to identify the underlying mechanism of action.

The BBB is composed of microvascular ECs and TJ proteins (Occludin, Claudins, and ZO) and adhesion junction proteins (VE-cadherin and PECAM-1) that interconnect with ECs (Citi and Cordenonsi, 1998; Stamatovic et al., 2008). TJ protein expression in brain ECs at a relatively high level, can maintain

the integrity of the BBB (Zhang et al., 2020), which is crucial for brain homeostasis. In contrast, disruption of BBB integrity correlates with reduced expression of TJ proteins such as Occludin, Claudin-5, and ZO (Nag et al., 2007; Williams et al., 2020). Mechanical stress associated with acute-stage TBI not only is detrimental to cells in the nervous system but also results in injury to the microvasculature in the brain, which consists of ECs, finally increasing paracellular permeability and causing a cascade of secondary damage to brain tissue (Alvarez et al., 2011). Therefore, we analyzed the protective effects of rhFGF20 on VE-cadherin, Occludin, and Claudin-5 expression in the brains of TBI mice and *in vitro* in TNF- $\alpha$  induced HBMECs by western blotting and immunofluorescence assays.

FGF20, expressed mainly in the brain, has been suggested to be a critical factor involved in brain development and neuronal homeostasis (Dono, 2003). Reports about the therapeutic effects of FGF20 on CNS conditions, except for PD and Alzheimer's disease (AD), are limited. FGF20 exerted a protective effect on dopamine neurons in a rat model of 6-hydroxydopamine-induced PD (Boshoff et al., 2018; Fletcher et al., 2019). However, the role of FGF20 in the BBB after TBI is unknown. In the present study, endogenous FGF20 levels were significantly decreased after TBI; this altered expression of endogenous FGF20 might be associated with TBI and could be beneficial in regulating the repair process. Therefore, the post-TBI protective effects of rhFGF20 on the BBB were explored. Considering that FGF20 cannot penetrate the BBB, it was administered by nasal delivery based on a previous study (Wang et al., 2016) before CCI-induced TBI; this method is a major limitation of this study. In subsequent studies, we will perform further experiments to adjust the time of the treatment window for FGF20 administration after TBI, which will make the findings more clinically meaningful.



In addition to being affected by primary damage resulting from the initial impact, alterations in BBB integrity can also be influenced by deleterious secondary injury responses, including inflammatory cascades and abnormal metabolic processes within the CNS (Maiti et al., 2019). These inflammatory factors supplement TJ destruction in the BBB (Ye et al., 2013). Several studies have reported that BBB dysfunction leads to a high degree of cerebral edema, increases the mortality rate and changes behavior (Xu et al., 2017; Chen et al., 2018).

Neuroinflammation involving the activation of microglia and astrocytes has been demonstrated to play a critical role in the secondary injury induced by TBI (Schober et al., 2019). In addition, treatment with FGF20 significantly inhibited the expression of Iba1 and GFAP markers of microglia and astrocyte activation, respectively 24 h after TBI. FGF functions through FGF receptor (FGFR) activation (Kalinina et al., 2009; Romero-Fernandez et al., 2011). Moreover, a previous study reported that FGFR1 also is expressed in astrocytes (Narvaez et al., 2020) and microglia (Tang et al., 2018) in the brain. A recent study reported that FGF21 suppressed microglia/macrophage-mediated neuroinflammation in stroke (Wang et al., 2020a). Herein, we speculated that FGF20 might have the

potential to regulate glial cells in order to control neuroinflammation in brain disease. However, the effect of FGF20 on glial cells and the underlying mechanism will be explored in our next work after we gain a better understanding of the protective effect of FGF20 after TBI. The AKT pathway is necessary for cell survival, and an increase in the  $p$ -AKT level protects against BBB damage after TBI (Wang et al., 2016). Phosphorylation of AKT decreases GSK3 activity (Zhao et al., 2006) by increasing the phosphorylation of GSK3 $\beta$ . Phosphorylation of GSK3 $\beta$  results in increased expression of neuroprotective and neurotrophic proteins (Ren et al., 2003) and brain-derived neurotrophic factor (BDNF) (Yasuda et al., 2009) and attenuates BBB recovery (Yu et al., 2012). Reports indicate that other FGFs can activate FGFR1 in ECs, regulate the AKT pathway, and exert cytoprotective effects (Huang et al., 2012). In the present study, we concluded that rhFGF20 increased the expression of junction proteins by activating the AKT/GSK3 $\beta$  pathway, and then preserved the function of the BBB. However, the precise mechanism by which FGF20 regulates the expression of junction proteins through the AKT/GSK3 $\beta$  pathway remains elusive. We speculate that several potential mechanisms, including increasing protein synthesis, regulating protein

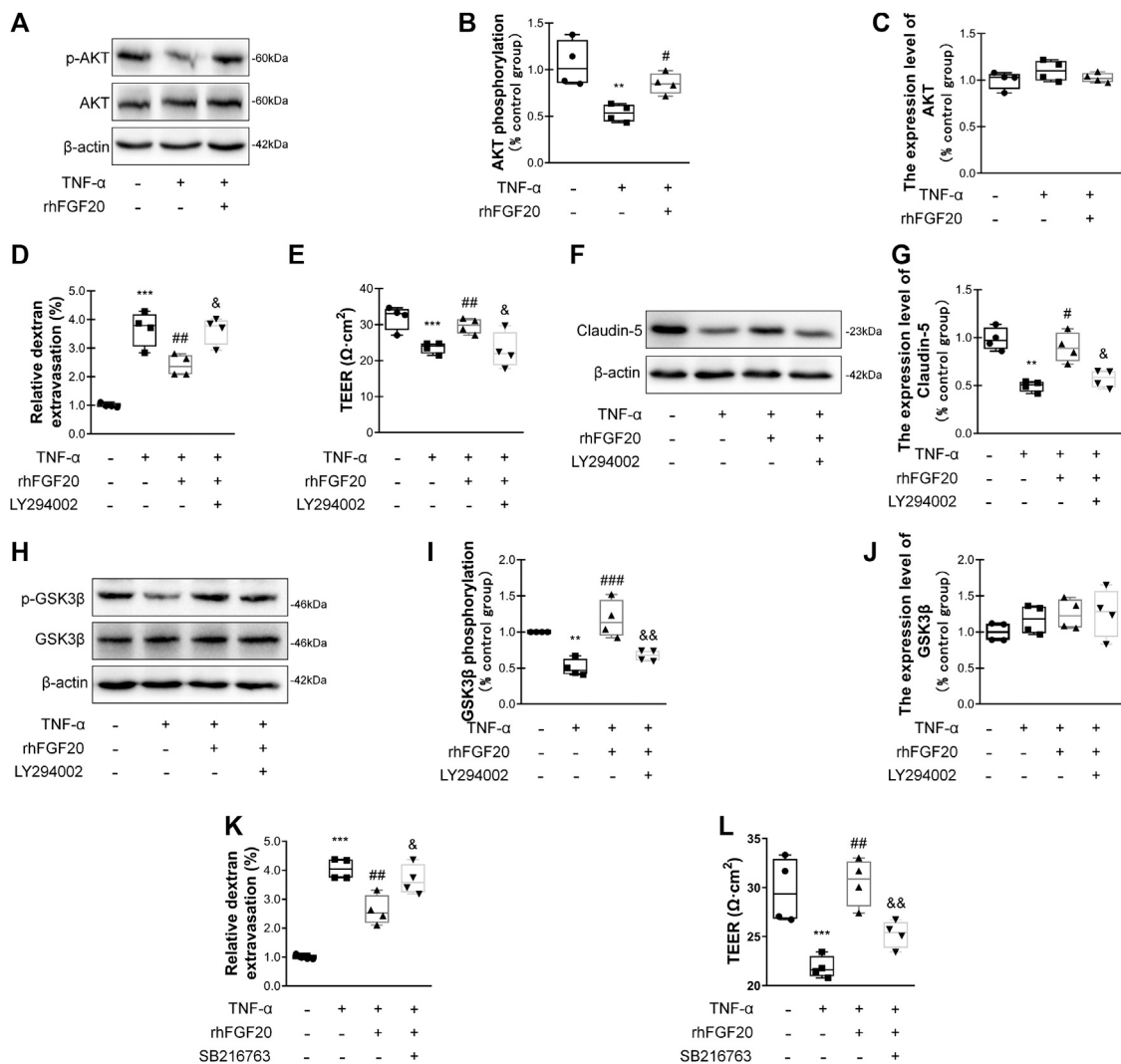
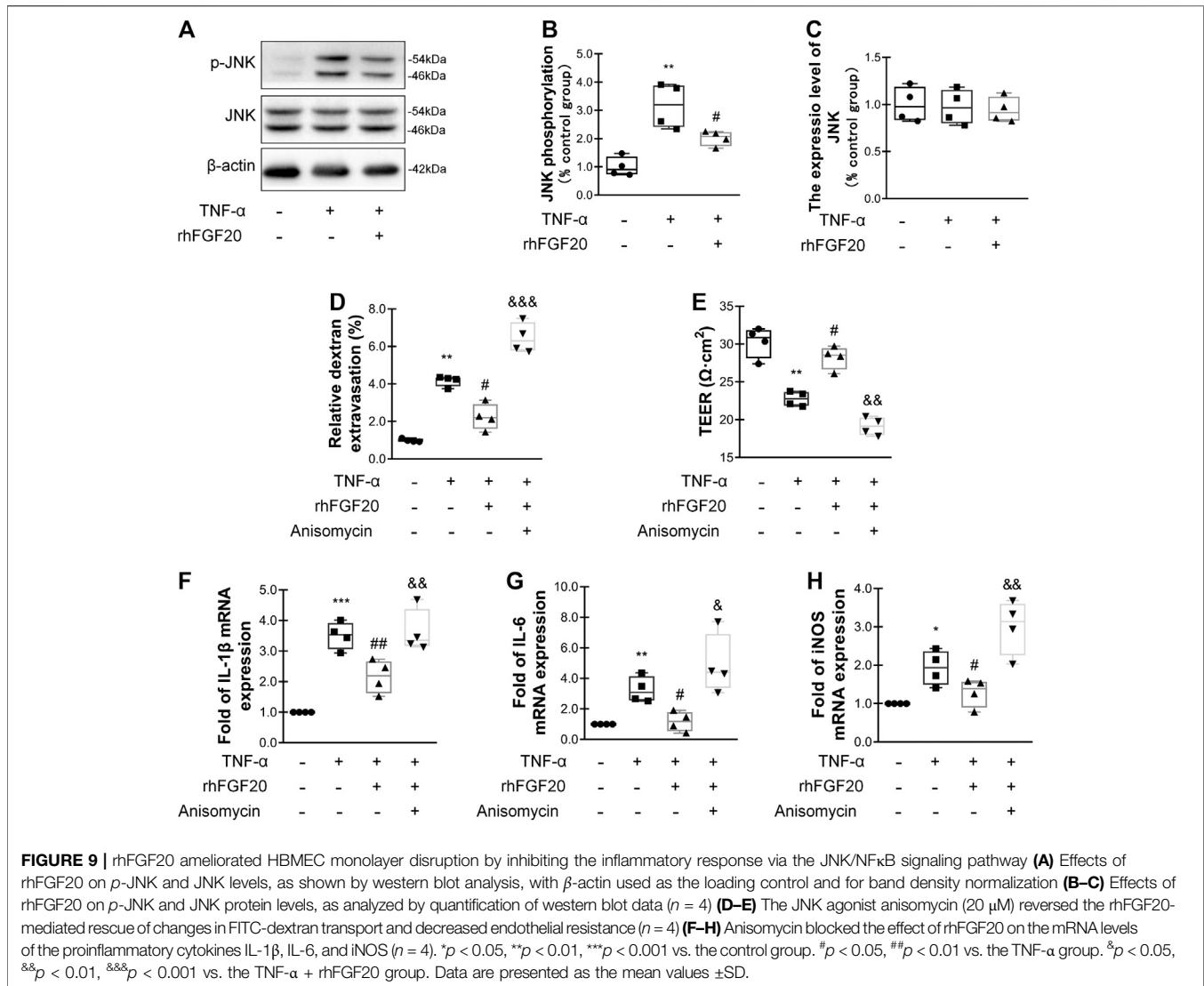


**FIGURE 8** | rhFGF20 ameliorated HBMEC monolayer disruption by increasing junction protein expression via AKT/GSK3 $\beta$  activation (A) Effects of rhFGF20 on p-AKT and AKT levels, as shown by western blot analysis of cellular protein, with  $\beta$ -actin used as the loading control and for band density normalization (B–C) Effects of rhFGF20 on p-AKT and AKT protein levels, as analyzed by quantification of western blot data ( $n = 4$ ) (D–E) The AKT inhibitor LY294002 (20  $\mu$ M) reversed the rhFGF20-mediated rescue of changes in FITC-dextran transport and decreased endothelial resistance ( $n = 4$ ) (F–G) LY294002 blocked the effect of rhFGF20 on Claudin-5 expression, as shown by western blot analysis of total cellular protein, with  $\beta$ -actin used as the loading control and for band density normalization ( $n = 4$ ) (H–J) Effects of rhFGF20 and LY294002 on p-GSK3 $\beta$  and GSK3 $\beta$  levels, as shown by western blot analysis of total cellular protein, with  $\beta$ -actin used as the loading control and for band density normalization ( $n = 4$ ) (K–L) The GSK3 $\beta$  inhibitor SB216763 (30  $\mu$ M) reversed the rhFGF20-mediated rescue of changes in FITC-dextran transport and decreased endothelial resistance ( $n = 4$ ). \*\* $p < 0.01$ , \*\*\* $p < 0.001$  vs. the control group. # $p < 0.05$ , ## $p < 0.01$ , ### $p < 0.001$  vs. the TNF- $\alpha$  group. & $p < 0.05$ , && $p < 0.01$  vs. TNF- $\alpha$  + rhFGF20 group. Data are presented as the mean values  $\pm$ SD.

modification and reducing protein degradation, may be involved, and we will explore and verify these mechanisms in the future.

Although more evidence is focused on BBB disruption after TBI, various factors affect BBB permeability, such as the animal species, the injury models, the severity of impact, and permeability measurements (Main et al., 2018). However, the extent and time of BBB permeability after TBI remain poorly understood. Main et al. (2018) thoroughly documented the extent and time of BBB permeability after TBI in different species and with detection methods. Acute BBB dysfunction appeared at 12–76 h with different measurement methods, and in some

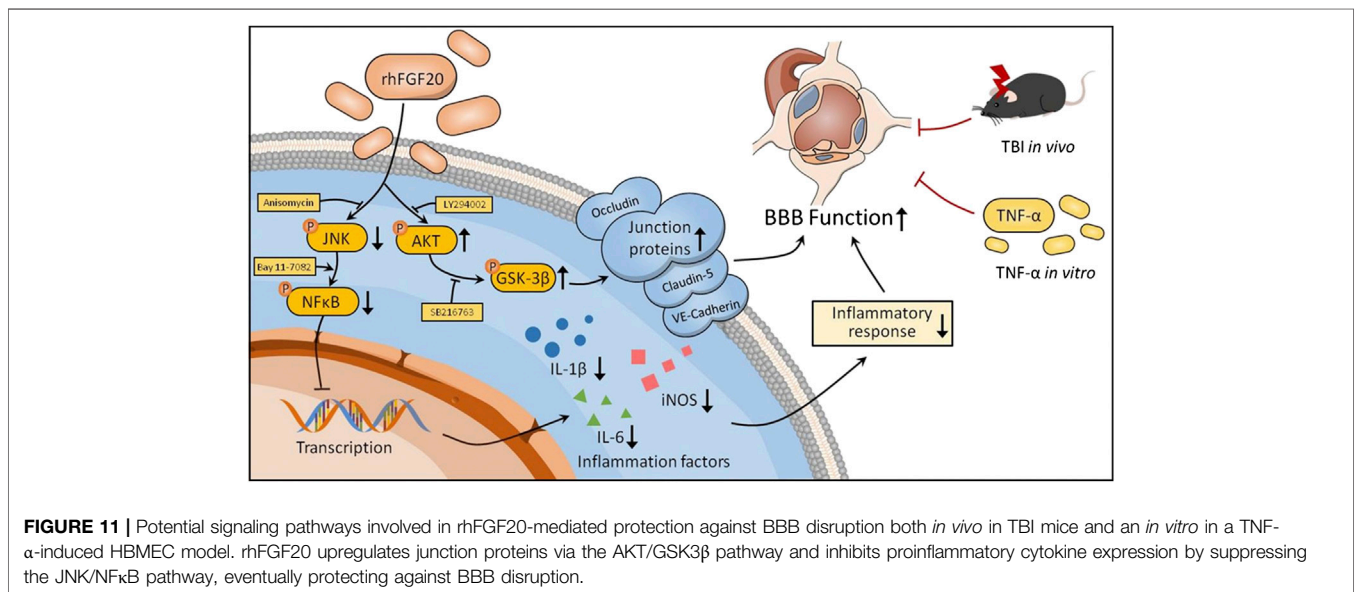
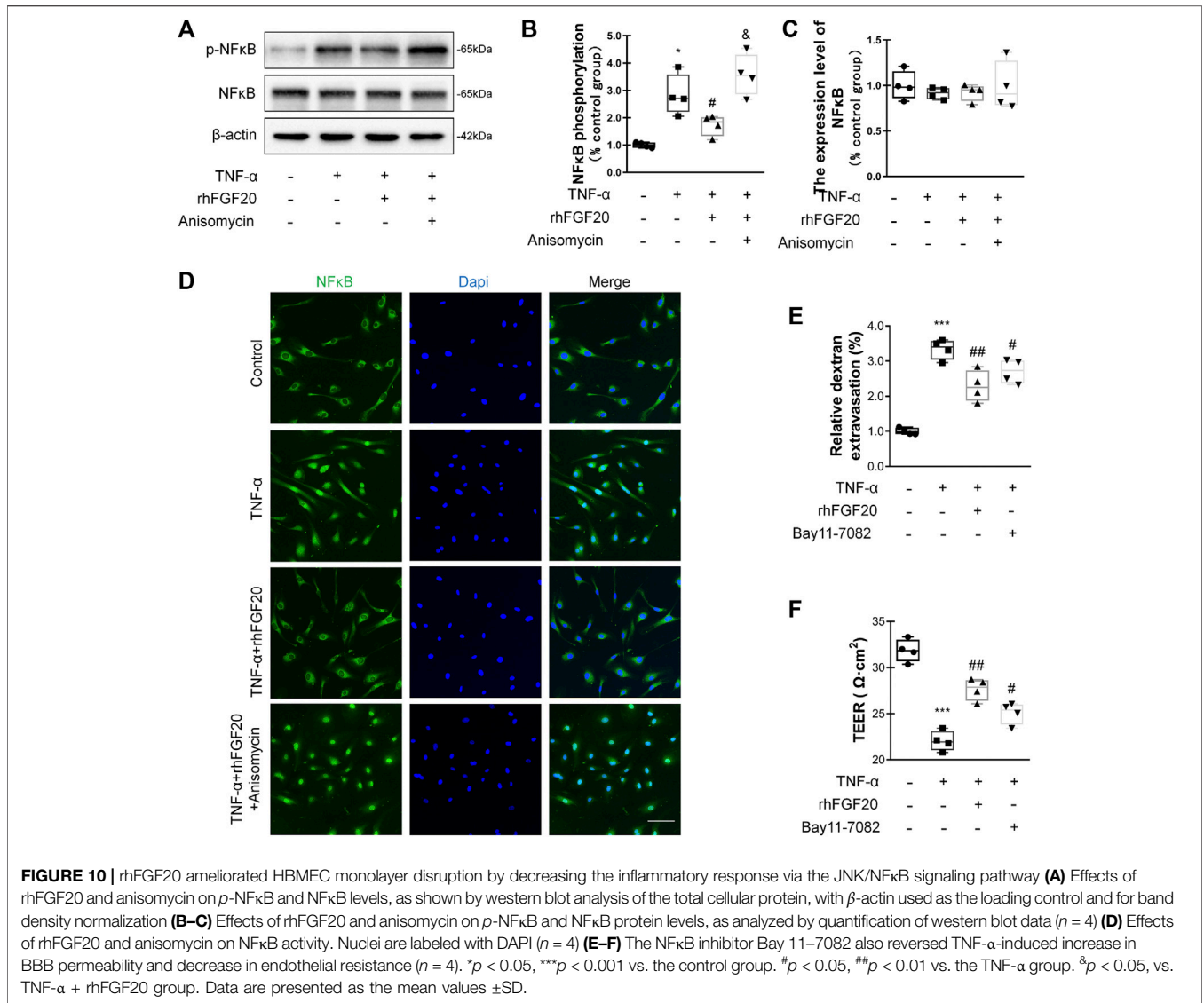
cases up to months or years post injury in humans. Rats exhibited BBB permeability at acute time points of 30 min–24 h, extending to 3 days after TBI in only a few individuals. Similarly, mouse models showed that acute BBB disruption began from 6 h and extended to 3 days; many pharmacological effects were evaluated at a single time point, most often 24 h post injury. In the present study, we established a CCI mouse model and explored the effects of rhFGF20 on TBI after 24 h of treatment. Our results showed that exogenous administration of rhFGF20 attenuated BBB disruption and the neuroinflammatory response in mice after TBI. In addition, rhFGF20 administration alleviated



cerebral edema and ameliorated functional behavior deficits after TBI.

Many mechanisms, including autophagy (Kim et al., 2020), endoplasmic reticulum stress (Xu et al., 2019), oxidative stress (Sharma et al., 2020) and so on, are involved in BBB damage. However, all of these mechanisms are related to inflammation, indicating that direct inhibition of inflammation also plays an important role in the repair of the BBB. We also found changes in cortical tissue post TBI and in TNF-induced HBMECs. In the TBI mouse model, rhFGF20 reduced the levels of inflammatory cytokines including IL-1β, IL-6, and iNOS. In addition, we further conducted *in vitro* model experiments and confirmed that FGF20 has a direct anti-inflammatory effect on TNF-α-induced ECs. The above results indicated that FGF20 can ameliorate ECs damage by inhibiting EC inflammation and then repair the BBB. In addition, we found that rhFGF20 markedly inhibited microglial activation in cortical tissue post TBI, as indicated by the reduced numbers of activated cells and somal areas, and increased ramified processes.

NFκB is a crucial transcription factor involved in the generation of the inflammatory response (Wang et al., 2020b). In addition, JNK is important for NFκB transactivation or translocation, which plays a pivotal role in inflammation process and constitutes an optimal therapeutic target for the pathogenesis of inflammation (Lan et al., 2019). We further explored whether the JNK signaling pathway was involved in the anti-inflammatory mechanism of rhFGF20. In the present study, administration of rhFGF20 to TBI mice and TNF-α-treated HBMECs decreased the level of p-JNK, and inhibited NF-κB activity and neuroinflammatory factor expression. Moreover, the JNK agonist anisomycin inhibited the anti-inflammatory effect of rhFGF20 and its ability to evoke repair of EC permeability. In addition, the NFκB inhibitor Bay11-7082 showed protective effects on EC permeability. Collectively, the above results demonstrated that rhFGF20 protected against BBB disruption by suppressing the inflammatory response, an effect that might be mediated through inhibition of the JNK and NF-κB signaling pathways. aFGF has been reported to inhibit the activity of JNK



and NF $\kappa$ B through TAK/TAB to exert anti-inflammatory effects, and FGF21 can inhibit the JNK/NF $\kappa$ B pathway (Lee et al., 2012); however this group did not mention activation of FGFR1. Therefore, we believe that FGF20 plays a protective role in ECs, and regulates the AKT pathway by activating FGFR1. In addition, FGF20 may also play a role in inhibiting the JNK signaling pathway through other receptors, a possibility that needs further study.

## CONCLUSION

In conclusion, these experimental findings demonstrated that treatment with exogenous rhFGF20 protected against BBB disruption by maintaining the integrity of TJ and AJ protein expression by activating the AKT/GSK3 $\beta$  pathway. In addition, rhFGF20 alleviated the cerebral inflammatory response by regulating the JNK/NF $\kappa$ B pathway, facilitating neurofunctional recovery and decreasing the degree of brain edema after TBI. These results were confirmed *in vitro* in TNF- $\alpha$  induced HBMECs (Figure 11). These findings extended our understanding of the effects of FGF20 in TBI treatment and suggested that FGF20 has potential clinical applications in cerebral endothelial barrier disruption-related disease and can be a therapeutic candidate for TBI.

## DATA AVAILABILITY STATEMENT

Publicly available datasets were analyzed in this study. This data can be found here: The raw data supporting the conclusions of this article will be made available by the authors, without undue reservation, to any qualified researcher.

## REFERENCES

- Abbott, N. J., Ronnback, L., and Hansson, E. (2006). Astrocyte-endothelial interactions at the blood-brain barrier. *Nat. Rev. Neurosci.* 7, 41–53. doi:10.1038/nrn1824
- Aibiki, M., Maekawa, S., Ogura, S., Kinoshita, Y., Kawai, N., et al. (1999). Effect of moderate hypothermia on systemic and internal jugular plasma IL-6 levels after traumatic brain injury in humans. *J. Neurotrauma.* 16, 225–232. doi:10.1089/neu.1999.16.225
- Alvarez, J. I., Dodelet-Devillers, A., Kebir, H., Ifergan, I., Fabre, P. J., et al. (2011). The Hedgehog pathway promotes blood-brain barrier integrity and CNS immune quiescence. *Science.* 334, 1727–1731. doi:10.1126/science.1206936
- Boshoff, E. L., Fletcher, E. J. R., and Duty, S. (2018). Fibroblast growth factor 20 is protective towards dopaminergic neurons *in vivo* in a paraffine manner. *Neuropharmacology.* 137, 156–163. doi:10.1016/j.neuropharm.2018.04.017
- Cernak, I. (2005). Animal models of head trauma. *NeuroRx.* 2, 410–422. doi:10.1602/neuroRx.2.3.410
- Chen, J., Hu, J., Liu, H., Xiong, Y., Zou, Y., et al. (2018). FGF21 protects the blood-brain barrier by upregulating PPAR $\gamma$  via FGFR1/ $\beta$ -klotho after traumatic brain injury. *J. Neurotrauma.* 35, 2091–2103. doi:10.1089/neu.2017.5271
- Chen, J., Wang, X., Hu, J., Huang, W., Dordoe, C., et al. (2020). FGF20 protected against BBB disruption after traumatic brain injury by activating the AKT/GSK3 $\beta$  pathway to upregulate junction protein expression and inhibiting JNK/NF $\kappa$ B-dependent neuroinflammation. *Res. Square [Preprint]*. doi:10.21203/rs.2.19529/v1
- Chen, X., Wu, S., Chen, C., Xie, B., Fang, Z., et al. (2017). Omega-3 polyunsaturated fatty acid supplementation attenuates microglial-induced inflammation by inhibiting the HMGB1/TLR4/NF- $\kappa$ B pathway following experimental traumatic brain injury. *J. Neuroinflammation.* 14, 143. doi:10.1186/s12974-017-0917-3
- Citi, S., and Cordenonsi, M. (1998). Tight junction proteins. *Biochim. Biophys. Acta.* 1448, 1–11. doi:10.1016/s0167-4889(98)00125-6
- Dono, R. (2003). Fibroblast growth factors as regulators of central nervous system development and function. *Am. J. Physiol. Regul. Integr. Comp. Physiol.* 284, R867–R881. doi:10.1152/ajpregu.00533.2002
- Elwood, E., Lim, Z., Naveed, H., and Galea, I. (2017). The effect of systemic inflammation on human brain barrier function. *Brain Behav. Immun.* 62, 35–40. doi:10.1016/j.bbi.2016.10.020
- Fletcher, E. J. R., Jamieson, A. D., Williams, G., Doherty, P., and Duty, S. (2019). Targeted repositioning identifies drugs that increase fibroblast growth factor 20 production and protect against 6-hydroxydopamine-induced nigra cell loss in rats. *Sci. Rep.* 9, 8336. doi:10.1038/s41598-019-44803-1
- Fouda, A. Y., Eldahshan, W., Narayanan, S. P., Caldwell, R. W., and Caldwell, R. B. (2020). Arginase pathway in acute retina and brain injury: therapeutic opportunities and unexplored avenues. *Front. Pharmacol.* 11, 277. doi:10.3389/fphar.2020.00277
- Garcia, J. H., Wagner, S., Liu, K. F., and Hu, X. J. (1995). Neurological deficit and extent of neuronal necrosis attributable to middle cerebral artery occlusion in rats. *Statistical validation.* *Stroke.* 26, 627–634. doi:10.1161/01.str.26.4.627
- Genet, G. F., Bentzer, P., Ostrowski, S. R., and Johansson, P. I. (2017). Resuscitation with pooled and pathogen-reduced plasma attenuates the increase in brain water content following traumatic brain injury and hemorrhagic shock in rats. *J. Neurotrauma.* 34, 1054–1062. doi:10.1089/neu.2016.4574
- Glushakov, A. V., Robbins, S. W., Bracy, C. L., and Narumiya, S. (2013). Prostaglandin F2 $\alpha$  FP receptor antagonist improves outcomes after

## ETHICS STATEMENT

The animal study was reviewed and approved by Laboratory Animal Centre, Wenzhou Medical University.

## AUTHOR CONTRIBUTIONS

LL and XL designed the experiments. JC and XW were involved in the design of the described experiments. JC, JH, WH, CD, KG, FH, and RG carried out the experiments. SY and JD analyzed data, QZ compiled the figures. JC and SY wrote the manuscript. XW and LL reviewed the manuscript. All authors read and approved the final manuscript.

## FUNDING

This work was supported by the by the National Natural Science Foundation of China (No. 81971180), Medical and Health Science and Technology Program of Zhejiang Province (2018KY505, WKJ-ZJ-2130), Natural Science Foundation of Zhejiang Province (LQ19H090012), CAMS Innovation Fund for Medical Sciences (2019-I2M-5-028), and Wenzhou Municipal Science and Technology Bureau (Y20170686).

## ACKNOWLEDGMENTS

We thank Prof. Zhifeng Huang (Wenzhou Medical University, Wenzhou, China) for providing rhFGF20. This manuscript has been released as a pre-print at [Research Square] (Chen et al., 2020).

- experimental traumatic brain injury. *J. Neuroinflammation*. 10, 132. doi:10.1186/1742-2094-10-132
- Graff, C. L., Zhao, R., and Pollack, G. M. (2005). Pharmacokinetics of substrate uptake and distribution in murine brain after nasal instillation. *Pharm. Res. (N. Y.)*. 22, 235–244. doi:10.1007/s11095-004-1191-5
- Huang, B., Krafft, P. R., Ma, Q., Rolland, W. B., Caner, B., et al. (2012). Fibroblast growth factors preserve blood-brain barrier integrity through RhoA inhibition after intracerebral hemorrhage in mice. *Neurobiol. Dis.* 46, 204–214. doi:10.1016/j.nbd.2012.01.008
- Jiao, H., Wang, Z., Liu, Y., Wang, P., and Xue, Y. (2011). Specific role of tight junction proteins claudin-5, occluding, and ZO-1 of the blood-brain barrier in a focal cerebral ischemic insult. *J. Mol. Neurosci.* 44, 130–139. doi:10.1007/s12031-011-9496-4
- Kalinina, J., Byron, S. A., Makarenkova, H. P., Olsen, S. K., Eliseenkova, A. V., et al. (2009). Homodimerization controls the fibroblast growth factor 9 subfamily's receptor binding and heparan sulfate-dependent diffusion in the extracellular matrix. *Mol. Cell Biol.* 29, 4663–4678. doi:10.1128/MCB.01780-08
- Kamm, K., Vanderkolk, W., Lawrence, C., Jonker, M., and Davis, A. T. (2006). The effect of traumatic brain injury upon the concentration and expression of interleukin-1beta and interleukin-10 in the rat. *J. Trauma*. 60, 152–157. doi:10.1097/01.ta.0000196345.81169.a1
- Katoh, M., and Katoh, M. (2005). Comparative genomics on FGF20 orthologs. *Oncol. Rep.* 14, 287–290.
- Kim, K. A., Kim, D., Kim, J. H., Shin, Y. J., Kim, E. S., et al. (2020). Autophagy-mediated occluding degradation contributes to blood-brain barrier disruption during ischemia in bEnd.3 brain endothelial cells and rat ischemic stroke models. *Fluids. Barriers. CNS*. 17, 21. doi:10.1186/s12987-020-00182-8
- Lan, Y. L., Wang, X., Zou, Y. J., Xing, J. S., Lou, J. C., et al. (2019). Bazedoxifene protects cerebral autoregulation after traumatic brain injury and attenuates impairments in blood-brain barrier damage: involvement of anti-inflammatory pathways by blocking MAPK signaling. *Inflamm. Res.* 68, 311–323. doi:10.1007/s00011-019-01217-z
- Lee, M. S., Choi, S. E., Ha, E. S., An, S. Y., Kim, T. H., et al. (2012). Fibroblast growth factor-21 protects human skeletal muscle myotubes from palmitate-induced insulin resistance by inhibiting stress kinase and NF-kappaB. *Metabolism*. 61, 1142–1151. doi:10.1016/j.metabol.2012.01.012
- Li, J. Y., Huang, J. Y., Li, M., Zhang, H., Xing, B., et al. (2012). Anisomycin induces glioma cell death via down-regulation of PP2A catalytic subunit *in vitro*. *Acta Pharmacol. Sin.* 33, 935–940. doi:10.1038/aps.2012.46
- Li, L., Shao, X., Cole, E. L., Ohnmacht, S. A., Ferrari, V., et al. (2015). Synthesis and initial *in Vivo* studies with ([11C]SB-216763: the first radiolabeled brain penetrative inhibitor of GSK-3. *ACS Med. Chem. Lett.* 6, 548–552. doi:10.1021/acsmchemlett.5b00044
- Li, X., Gao, J., Ding, J., Hu, G., and Xiao, M. (2013). Aquaporin-4 expression contributes to decreases in brain water content during mouse postnatal development. *Brain Res. Bull.* 94, 49–55. doi:10.1016/j.brainresbull.2013.02.004
- Lin, L., Wang, Q., Qian, K., Cao, Z., Xiao, J., et al. (2018). bFGF protects against oxygen glucose deprivation/reoxygenation-induced endothelial monolayer permeability via S1PR1-dependent mechanisms. *Mol. Neurobiol.* 55, 3131–3142. doi:10.1007/s12035-017-0544-0
- Loane, D. J., and Faden, A. I. (2010). Neuroprotection for traumatic brain injury: translational challenges and emerging therapeutic strategies. *Trends Pharmacol. Sci.* 31, 596–604. doi:10.1016/j.tips.2010.09.005
- Lu, S., Luo, Y., Zhou, P., Yang, K., Sun, G., et al. (2019). Ginsenosides compound K protects human umbilical vein endothelial cells against oxidized low-density lipoprotein-induced injury via inhibition of nuclear factor-kappaB, p38, and JNK MAPK pathways. *J. Ginseng. Res.* 43, 95–104. doi:10.1016/j.jgr.2017.09.004
- Main, B. S., Villapol, S., Sloley, S. S., Barton, D. J., Parsadanian, M., et al. (2018). Apolipoprotein E4 impairs spontaneous blood brain barrier repair following traumatic brain injury. *Mol. Neurodegener.* 13, 17. doi:10.1186/s13024-018-0249-5
- Maiti, P., Peruzzaro, S., Kolli, N., Andrews, M., Al-Gharaibeh, A., Rossignol, J., et al. (2019). Transplantation of mesenchymal stem cells overexpressing interleukin-10 induces autophagy response and promotes neuroprotection in a rat model of TBI. *J. Cell Mol. Med.* 23, 5211–5224. doi:10.1111/jcmm.14396
- Nag, S., Venugopalan, R., and Stewart, D. J. (2007). Increased caveolin-1 expression precedes decreased expression of occluding and claudin-5 during blood-brain barrier breakdown. *Acta Neuropathol.* 114, 459–469. doi:10.1007/s00401-007-0274-x
- Narvaez, M., Andrade-Talavera, Y., Valladolid-Acebes, I., Fredriksson, M., Siegle, P., et al. (2020). Existence of FGFR1-5-HT1AR heteroreceptor complexes in hippocampal astrocytes. Putative link to 5-HT and FGF2 modulation of hippocampal gamma oscillations. *Neuropharmacology*. 170, 108070. doi:10.1016/j.neuropharm.2020.108070
- Niu, J., Xie, J., Guo, K., Zhang, X., Xia, F., et al. (2018). Efficient treatment of Parkinson's disease using ultrasonography-guided rhFGF20 proteoliposomes. *Drug Deliv.* 25, 1560–1569. doi:10.1080/10717544.2018.1482972
- Odobasic, D., Oudin, V., Ito, K., Gan, P. Y., Kitching, A. R., et al. (2019). Tolerogenic dendritic cells attenuate experimental autoimmune antemyeloperoxidase glomerulonephritis. *J. Am. Soc. Nephrol.* doi:10.1681/ASN.2019030236
- Ohmachi, S., Watanabe, Y., Mikami, T., Kusu, N., Ibi, T., et al. (2000). FGF-20, a novel neurotrophic factor, preferentially expressed in the substantia nigra pars compacta of rat brain. *Biochem. Biophys. Res. Commun.* 277, 355–360. doi:10.1006/bbrc.2000.3675
- Peterson, T. C., Maass, W. R., Anderson, J. R., Anderson, G. D., and Hoane, M. R. (2015). A behavioral and histological comparison of fluid percussion injury and controlled cortical impact injury to the rat sensorimotor cortex. *Behav. Brain Res.* 294, 254–263. doi:10.1016/j.bbr.2015.08.007
- Polderman, K. H. (2004). Application of therapeutic hypothermia in the ICU: opportunities and pitfalls of a promising treatment modality. Part 1: indications and evidence. *Intensive Care Med.* 30, 556–575. doi:10.1007/s00134-003-2152-x
- Ren, M., Senatorov, V. V., Chen, R. W., and Chuang, D. M. (2003). Postsult treatment with lithium reduces brain damage and facilitates neurological recovery in a rat ischemia/reperfusion model. *P. Natl. Acad. Sci. USA*. 100, 6210–6215. doi:10.1073/pnas.0937423100
- Rochfort, K. D., and Cummins, P. M. (2015). Cytokine-mediated dysregulation of zonula occludens-1 properties in human brain microvascular endothelium. *Microvasc. Res.* 100, 48–53. doi:10.1016/j.mvr.2015.04.010
- Romero-Fernandez, W., Borroto-Escuela, D. O., Tarakanov, A. O., Mudo, G., Narvaez, M., et al. (2011). Agonist-induced formation of FGFR1 homodimers and signaling differ among members of the FGF family. *Biochem. Biophys. Res. Commun.* 409, 764–768. doi:10.1016/j.bbrc.2011.05.085
- Schober, M. E., Requena, D. F., Casper, T. C., Velhorst, A. K., Lolofie, A., et al. (2019). Docosahexaenoic acid decreased neuroinflammation in rat pups after controlled cortical impact. *Exp. Neurol.* 320, 112971. doi:10.1016/j.expneurol.2019.112971
- Shahror, R. A., Linares, G. R., Wang, Y., Hsueh, S. C., Wu, C. C., et al. (2020). Transplantation of mesenchymal stem cells overexpressing fibroblast growth factor 21 facilitates cognitive recovery and enhances neurogenesis in a mouse model of traumatic brain injury. *J. Neurotrauma*. 37, 14–26. doi:10.1089/neu.2019.6422
- Sharma, R., Kambhampati, S. P., Zhang, Z., Sharma, A., Chen, S., et al. (2020). Dendrimer mediated targeted delivery of sinomenine for the treatment of acute neuroinflammation in traumatic brain injury. *J. Contr. Release.* 323, 361–375. doi:10.1016/j.jconrel.2020.04.036
- Shi, H., Wang, H. L., Pu, H. J., Shi, Y. J., Zhang, J., et al. (2015). Ethyl pyruvate protects against blood-brain barrier damage and improves long-term neurological outcomes in a rat model of traumatic brain injury. *CNS Neurosci. Ther.* 21, 374–384. doi:10.1111/cns.12366
- Shimada, H., Yoshimura, N., Tsuji, A., and Kunisada, T. (2009). Differentiation of dopaminergic neurons from human embryonic stem cells: modulation of differentiation by FGF-20. *J. Biosci. Bioeng.* 107, 447–454. doi:10.1016/j.jbiosc.2008.12.013
- Shlosberg, D., Benifla, M., Kaufer, D., and Friedman, A. (2010). Blood-brain barrier breakdown as a therapeutic target in traumatic brain injury. *Nat. Rev. Neurol.* 6, 393–403. doi:10.1038/nrnneurol.2010.74
- Simon, D. W., McGeachy, M. J., Bayir, H., Clark, R. S., Loane, D. J., et al. (2017). The far-reaching scope of neuroinflammation after traumatic brain injury. *Nat. Rev. Neurol.* 13, 171–191. doi:10.1038/nrnneurol.2017.13
- Stamatovic, S. M., Keep, R. F., and Andjelkovic, A. V. (2008). Brain endothelial cell-cell junctions: how to "open" the blood brain barrier. *Curr. Neuropharmacol.* 6, 179–192. doi:10.2174/157015908785777210
- Takagi, Y., Takahashi, J., Saiki, H., Morizane, A., Hayashi, T., et al. (2005). Dopaminergic neurons generated from monkey embryonic stem cells function in a Parkinson primate model. *J. Clin. Invest.* 115, 102–109. doi:10.1172/JCI21137

- Tang, M. M., Lin, W. J., Pan, Y. Q., and Li, Y. C. (2018). Fibroblast growth factor 2 modulates hippocampal microglia activation in a neuroinflammation induced model of depression. *Front. Cell. Neurosci.* 12, 255. doi:10.3389/fncel.2018.00255
- Vigo, M. B., Perez, M. J., De Fino, F., Gomez, G., Martinez, S. A., et al. (2019). Acute acetaminophen intoxication induces direct neurotoxicity in rats manifested as astrogliosis and decreased dopaminergic markers in brain areas associated with locomotor regulation. *Biochem. Pharmacol.* 170, 113662. doi:10.1016/j.bcp.2019.113662
- Villalba, N., Sonkusare, S. K., Longden, T. A., Tran, T. L., Sackheim, A. M., et al. (2014). Traumatic brain injury disrupts cerebrovascular tone through endothelial inducible nitric oxide synthase expression and nitric oxide gain of function. *J. Am. Heart Assoc.* 3, e001474. doi:10.1161/JAHA.114.001474
- Wang, D., Liu, F., Zhu, L., Lin, P., Han, F., et al. (2020a). FGF21 alleviates neuroinflammation following ischemic stroke by modulating the temporal and spatial dynamics of microglia/macrophages. *J. Neuroinflammation.* 17, 257. doi:10.1186/s12974-020-01921-2
- Wang, X., Zhu, L. Y., Hu, J., Guo, R. L., Ye, S. S., et al. (2020b). viaFGF21 attenuated LPS-induced depressive-like behavior inhibiting the inflammatory pathway. *Front. Pharmacol.* 11, 154. doi:10.3389/fphar.2020.00154
- Wang, Z. G., Cheng, Y., Yu, X. C., Ye, L. B., and Xia, Q. H. (2016). bFGF protects against blood-brain barrier damage through junction protein regulation via PI3K-Akt-Rac1 pathway following traumatic brain injury. *Mol. Neurobiol.* 53, 7298–7311. doi:10.1007/s12035-015-9583-6
- Williams, A. M., Bhatti, U. F., Brown, J. F., Biesterveld, B. E., Kathawate, R. G., et al. (2020). Early single-dose treatment with exosomes provides neuroprotection and improves blood-brain barrier integrity in swine model of traumatic brain injury and hemorrhagic shock. *J. Trauma Acute Care.* 88, 207–218. doi:10.1097/TA.0000000000002563
- Wolburg, H., and Lippoldt, A. (2002). Tight junctions of the blood-brain barrier: development, composition and regulation. *Vasc. Pharmacol.* 38, 323–337. doi:10.1016/s1537-1891(02)00200-8
- Wu, F., Xu, K., Xu, K., Teng, C., Zhang, M., et al. (2020). DI-3n-butylphthalide improves traumatic brain injury recovery via inhibiting autophagy-induced blood-brain barrier disruption and cell apoptosis. *J. Cell Mol. Med.* 24, 1220–1232. doi:10.1111/jcmm.14691
- Xu, W., Li, T., Gao, L., Zheng, J., Yan, J., et al. (2019). Apelin-13/APJ system attenuates early brain injury via suppression of endoplasmic reticulum stress-associated TXNIP/NLRP3 inflammasome activation and oxidative stress in a AMPK-dependent manner after subarachnoid hemorrhage in rats. *J. Neuroinflammation.* 16, 247. doi:10.1186/s12974-019-1620-3
- Xu, X., Yin, D., Ren, H., Gao, W., and Li, F. (2018). Selective NLRP3 inflammasome inhibitor reduces neuroinflammation and improves long-term neurological outcomes in a murine model of traumatic brain injury. *Neurobiol. Dis.* 117, 15–27. doi:10.1016/j.nbd.2018.05.016
- Xu, Z. M., Yuan, F., Liu, Y. L., Ding, J., and Tian, H. L. (2017). Glibenclamide attenuates blood-brain barrier disruption in adult mice after traumatic brain injury. *J. Neurotrauma.* 34, 925–933. doi:10.1089/neu.2016.4491
- Yan, H. Q., Yu, J., Kline, A. E., Letart, P., Jenkins, L. W., et al. (2000). Evaluation of combined fibroblast growth factor-2 and moderate hypothermia therapy in traumatically brain injured rats. *Brain Res.* 887, 134–143. doi:10.1016/s0006-8993(00)03002-x
- Yasuda, S., Liang, M. H., Marinova, Z., Yahyavi, A., and Chuang, D. M. (2009). The mood stabilizers lithium and valproate selectively activate the promoter IV of brain-derived neurotrophic factor in neurons. *Mol. Psychiatr.* 14, 51–59. doi:10.1038/sj.mp.4002099
- Ye, L., Huang, Y., Zhao, L., Li, Y., Sun, L., et al. (2013). IL-1beta and TNF-alpha induce neurotoxicity through glutamate production: a potential role for neuronal glutaminase. *J. Neurochem.* 125, 897–908. doi:10.1111/jnc.12263
- Yoshimura, S., Teramoto, T., Whalen, M. J., Irizarry, M. C., Takagi, Y., et al. (2003). FGF-2 regulates neurogenesis and degeneration in the dentate gyrus after traumatic brain injury in mice. *J. Clin. Invest.* 112, 1202–1210. doi:10.1172/JCI16618
- Yu, F., Wang, Z., Tchantchou, F., Chiu, C. T., Zhang, Y., et al. (2012). Lithium ameliorates neurodegeneration, suppresses neuroinflammation, and improves behavioral performance in a mouse model of traumatic brain injury. *J. Neurotrauma.* 29, 362–374. doi:10.1089/neu.2011.194
- Zhang, L. L., Xu, S. S., Wu, X. X., Chen, J. O., Guo, X. L., et al. (2020). Combined treatment with 2-(2-benzofury-2-yl)-2-imidazoline and recombinant tissue plasminogen activator protects blood-brain barrier integrity in a rat model of embolic middle cerebral artery occlusion. *Front. Pharmacol.* 11, 801. doi:10.3389/fphar.2020.00801
- Zhang, X., Du, Q., Yang, Y., Wang, J., Liu, Y., et al. (2018). Salidroside alleviates ischemic brain injury in mice with ischemic stroke through regulating BDNF mediated PI3K/Akt pathway. *Biochem. Pharmacol.* 156, 99–108. doi:10.1016/j.bcp.2018.08.015
- Zhao, H., Sapolsky, R. M., and Steinberg, G. K. (2006). Phosphoinositide-3-kinase/akt survival signal pathways are implicated in neuronal survival after stroke. *Mol. Neurobiol.* 34, 249–270. doi:10.1385/MN:34:3:249
- Zhao, Q., Zhang, F., Yu, Z., Guo, S., Liu, N., et al. (2019). HDAC3 inhibition prevents blood-brain barrier permeability through Nrf2 activation in type 2 diabetes male mice. *J. Neuroinflammation.* 16, 103. doi:10.1186/s12974-019-1495-3
- Zhou, Y., Ming, J., Li, Y., Deng, M., Chen, Q., et al. (2019). Ligustilide attenuates nitric oxide-induced apoptosis in rat chondrocyte and cartilage degradation via inhibiting JNK and p38 MAPK pathways. *J. Cell Mol. Med.* 23, 3357–3368. doi:10.1111/jcmm.14226
- Zhu, L., Lin, M., Ma, J., Liu, W., Gao, L., et al. (2019). The role of LINC00094/miR-224-5p (miR-497-5p)/Endophilin-1 axis in Memantine mediated protective effects on blood-brain barrier in AD microenvironment. *J. Cell Mol. Med.* 23, 3280–3292. doi:10.1111/jcmm.14214

**Conflict of Interest:** The authors declare that the research was conducted in the absence of any commercial or financial relationships that could be construed as a potential conflict of interest.

Copyright © 2021 Chen, Wang, Hu, Du, Dordoe, Zhou, Huang, Guo, Han, Guo, Ye, Lin and Li. This is an open-access article distributed under the terms of the Creative Commons Attribution License (CC BY). The use, distribution or reproduction in other forums is permitted, provided the original author(s) and the copyright owner(s) are credited and that the original publication in this journal is cited, in accordance with accepted academic practice. No use, distribution or reproduction is permitted which does not comply with these terms.